

Transition from a Dirac spin liquid to an antiferromagnet: Monopoles in a QED₃-Gross-Neveu theory

Éric Dupuis,¹ M.B. Paranjape,^{1,2} and William Witczak-Krempa^{1,2}

¹*Département de physique, Université de Montréal, Montréal (Québec), H3C 3J7, Canada*

²*Centre de Recherches Mathématiques, Université de Montréal; P.O. Box 6128, Centre-ville Station; Montréal (Québec), H3C 3J7, Canada*

(Dated: March 18, 2022)

We study the quantum phase transition from a Dirac spin liquid to an antiferromagnet driven by condensing monopoles with spin quantum numbers. We describe the transition in field theory by tuning a fermion interaction to condense a spin-Hall mass, which in turn allows the appropriate monopole operators to proliferate and confine the fermions. We compute various critical exponents at the quantum critical point (QCP), including the scaling dimensions of monopole operators by using the state-operator correspondence of conformal field theory. We find that the degeneracy of monopoles in QED₃ is lifted and yields a non-trivial monopole hierarchy at the QCP. In particular, the lowest monopole dimension is found to be smaller than that of QED₃ using a large N_f expansion where $2N_f$ is the number of fermion flavors. For the minimal magnetic charge, this dimension is $0.39N_f$ at leading order. We also study the QCP between Dirac and chiral spin liquids, which allows us to test a conjectured duality to a bosonic CP¹ theory. Finally, we discuss the implications of our results for quantum magnets on the Kagome lattice.

Contents		
		B. Antiferromagnetic order parameter 19
		C. Quantum phase transition 20
I. Introduction	1	VIII. Conclusion 21
II. Preliminaries	3	Acknowledgments 21
A. Monopole operators in QED ₃	3	References 21
B. Confinement-deconfinement transition to an antiferromagnet	3	A. Regularization of the integrated logarithm 24
1. Spin-Hall mass condensation in the $1/N_f$ expansion	4	B. Saddle point equations for QED₃ – cHGN in a thermal setup 24
III. Scaling dimensions of monopole operators	4	C. Feynman diagrams computation 25
A. State-operator correspondence and $1/N_f$ expansion	5	1. Feynman rules 26
B. Spectrum of the Dirac operator with a spin-Hall mass	5	2. Computation of one-loop Feynman diagrams 26
C. Scaling dimension computation	7	a. Three-point functions 26
D. Monopole scaling dimensions for large q	9	b. Two-point functions 27
IV. Monopole dressing	9	c. Four-point function 28
V. Comparison with SU($2N_f$) symmetric critical point	11	d. Mass perturbations 29
A. Testing a duality with bosonic CP ¹ model	12	3. Results 29
VI. Renormalization group analysis of the critical fixed point	13	
A. Setup	14	I. INTRODUCTION
B. Fixed points in the $1/N_f$ expansion	14	Quantum spin liquids (QSLs) are strongly correlated phases of matter characterized by long-range entanglement, fractionalized excitations and, in some cases, topological order [1–3]. QSLs can arise in frustrated antiferromagnets where important quantum fluctuations lead to a highly entangled and non-magnetic ground state. In recent years, many candidate materials that may realize a QSL have been identified [3–7].
C. RG study in the $\epsilon = 4 - d$ expansion	15	
1. Critical exponents at the quantum critical point	15	
VII. Quantum phase transition in the Kagome magnet	18	
A. Emergent QED ₃	18	

The fractionalized excitations of a QSL are said to be deconfined as they don't appear in ordered phases. One important aspect to better understand the fractionalized aspect of these phases of matter is to characterize their transition to confined phases, that is to characterize confinement-deconfinement phase transitions. In this respect, the U(1) Dirac spin liquid (DSL) or algebraic spin liquid, which potentially describes certain two-dimensional QSLs at low energy, is an interesting example. This theory corresponds to quantum electrodynamics in $2 + 1$ dimensions (QED_3) with typically $2N_f = 4$ massless fermions, called spinons, and an emergent U(1) gauge field. The U(1) gauge field is compact given the underlying lattice, and for this reason the spectrum of the DSL contains topological disorder operators known as monopole operators. These are the operators that may drive confinement. In a pure compact U(1) gauge theory, monopoles proliferate and confine the gauge field [8]. The presence of massless fermions may screen the monopoles and prevent the confinement given a sufficiently large number of fermion flavors [9]. The stability of a QSL is thus determined by the relevance of monopole operators. Even if the spin liquid is intrinsically stable, monopole operators may still drive confinement if the fermions are gapped out at a phase transition. This is the situation considered in this paper.

The DSL phase has been used to describe quantum magnets in many contexts. On the triangular lattice, variational Monte Carlo (VMC) studies [10; 11] have shown that the ground state of a $J_1 - J_2$ Heisenberg antiferromagnet in the range $0.07 < J_2/J_1 < 0.15$ is given by the DSL. VMC studies [12–15] and other numerical methods [16; 17] also favor a DSL as the ground state of an Heisenberg antiferromagnet on the Kagome lattice. These results are not yet firmly established as contradicting studies find gapped spin liquids in both these contexts. The transition to a confined phase through monopole condensation was proposed for the DSL on the square lattice by Ghaemi and Senthil in Ref. [18]. A certain class of monopole operators with spin quantum numbers may also give the correct order parameter for the $\mathbf{q} = 0$ antiferromagnet on the Kagome lattice [19].

Topological disorder operators such as the monopole operators play an important role in other contexts. For example, they are involved in the physics of deconfined quantum critical points (dQCPs) [20; 21]. The prototypical case study is the quantum critical point of the Néel-VBS phase transition on the square lattice which is described by the bosonic CP^1 theory where the condensation of monopole operators which have lattice quantum numbers allows this non-Landau phase transition. The properties of the monopole operators in the CP^1 theory have been studied numerically in Refs. [22–24]. It is also important to note that dQCPs correspond to strongly correlated systems whose description may be reformulated as field theoretical dualities. A well known example is the particle-vortex duality [25; 26]. Recently, many new dualities have been found in $2 + 1$ dimensional

gauge theories (earlier examples of this resurgence can be found in Refs. [27–29]). Studying critical properties of topological disorder operators provides useful data which may serve to verify conjectured dualities. Confinement-deconfinement transitions are also important in particle physics where the confinement of quarks into hadrons at low energy is a long-standing issue. In fact, the original motivation of Polyakov to study compact QED_3 was to obtain a toy model of confinement of quantum chromodynamics. These relations to deep advancements in quantum phases of matter and quantum field theories motivate further our study of monopole operators.

The objective of this paper is to provide a field theoretical characterization of the confinement-deconfinement transition from a DSL to an antiferromagnetic phase. We will study the properties of a quantum critical point (QCP) separating these phases, which is in fact a conformal field theory. The transition will be described with a Gross-Neveu like deformation of QED_3 , where a fermion mass is condensed by tuning a fermion interaction. In turn, the gapped fermions no longer screen the monopole operators which can proliferate. Special attention is given to these topological operators. The central result of our work is the scaling dimension of monopole operators at the QCP. The field theory used to describe this confinement-deconfinement transition with the condensation of a spin-Hall mass was proposed in Ref. [30]. The idea was later generalized to include the condensation of any monopole operator following the condensation of an appropriate fermion bilinear [31].

The paper is structured as follows. In Sec. II, we give the theoretical background for the monopole operators and the confinement-deconfinement transition driven by the condensation of a spin-Hall mass. In Sec. III, we compute the lowest scaling dimension of monopole operators at the QCP using the state-operator correspondence. We find that the monopole scaling dimension is lower at the QCP than at the QED_3 fixed point. We also obtain an analytical approximation of the scaling dimension in the limit of large magnetic charge. In Sec. IV, we consider distinct fermionic dressings that define monopole operators with various quantum numbers, and show there is a hierarchy in the related scaling dimensions. We also discuss the role of these distinct monopole flavors when constructing perturbations allowed by lattice symmetries. In Sec. V, we do the same analysis in a transition to a chiral spin liquid, where a mass respecting the full flavor group is condensed instead of a spin-Hall mass. Extrapolating our results to $2N_f = 2$ allows us to test the duality between the QED_3 -Gross-Neveu QCP and the bosonic CP^1 theory. In Sec. VI, we do a one-loop perturbative renormalization group analysis of the non-compact field theory describing the confinement-deconfinement transition. We find an infrared fixed point corresponding to the QCP and we compute various critical exponents. In Sec. VII, we discuss the implications of our results for the phase transition in the particular case of the Kagome Heisenberg lattice model. We summarize our results and

discuss directions for future research in Sec. VIII.

II. PRELIMINARIES

A. Monopole operators in QED₃

Let us consider QED₃ with $2N_f$ flavors of massless two-component Dirac fermions, ψ_A where $A = 1, 2, \dots, 2N_f$. The flavors could correspond to magnetic spin and valley degrees of freedom, see Sec. VII for a discussion of how they arise in the Kagome Heisenberg model. These fermions can be organized as a spinor in flavor space, $\Psi = (\psi_1, \psi_2, \dots, \psi_{2N_f})^\top$. In Euclidean signature, the bare action reads

$$S_{\text{QED}_3} = \int d^3x \left[-\bar{\Psi} \not{D}_a \Psi + \frac{1}{2e^2} (\epsilon_{\mu\nu\rho} \partial_\nu a_\rho)^2 \right] \quad (1)$$

where a_μ is the U(1) gauge field, $\bar{\Psi} = \Psi^\dagger \gamma_0$ and \not{D}_a is the gauge covariant derivative

$$\not{D}_a \Psi = \gamma_\mu (\partial_\mu - ia_\mu) \Psi. \quad (2)$$

The Dirac matrices γ_μ act on Lorentz spinor components and realize a two-dimensional representation of the Clifford algebra, $\{\gamma_\mu, \gamma_\nu\} = 2\delta_{\mu\nu} \mathbb{1}_2$. They can be chosen as $\gamma_\mu = (\tau_3, \tau_2, -\tau_1)$ where the τ_i are the Pauli matrices.

As it is written in Eq. (1), QED₃ has a global symmetry, $U(1)_{\text{top}}$, which is related to the conservation of the magnetic current $j_{\text{top}}^\mu(x) = \frac{1}{2\pi} \epsilon^{\mu\nu\rho} \partial_\nu a_\rho(x)$. In the lattice regularization of this theory, it may no longer be the case that this current is conserved. Indeed, in the compact version of QED₃, a_μ is a periodic gauge field which takes values in the compact U(1) gauge group. This implies 2π quantization of the magnetic flux and the existence of instantons called monopole operators in this context. These operators insert integer multiples of the flux quantum and break the $U(1)_{\text{top}}$ symmetry. Non-compact QED₃ may still describe correctly the infrared (IR) limit of compact QED₃ if monopole operators are irrelevant. The theory is then said to exhibit an emergent $U(1)_{\text{top}}$ global symmetry in the infrared. Unless stated otherwise, we mean compact QED₃ when we simply write QED₃ throughout the paper.

Let $\mathcal{M}_q^\dagger(x)$ be a monopole operator with a $U(1)_{\text{top}}$ charge q at spacetime point x such that $2q \in \mathbb{Z}$. This disorder operator inserts a $4\pi q$ magnetic flux. More precisely, the Operator Product Expansion (OPE) of the magnetic current operator and the monopole operator yields the expected magnetic field for a magnetic monopole with charge q [9]

$$j_{\text{top}}^\mu(x) \mathcal{M}_q^\dagger(0) \sim \frac{q}{4\pi} \frac{x^\mu}{|x|^3} \mathcal{M}_q^\dagger(0) + \dots, \quad (3)$$

where the ellipsis denotes less singular terms as $|x| \rightarrow 0$. Apart from the magnetic flux they insert, another important property defining monopole operators is their gauge

invariance. In particular, these operators must have a vanishing fermionic number. Among U(1) gauge invariant $4\pi q$ -flux inserting operators, monopole operators are the most relevant, that is, they have the lowest scaling dimension. Only certain fermionic occupations can produce such operators: Among the $4qN_f$ fermion zero modes existing in the monopole background [32], half of them must be filled. There are many ways to satisfy this condition, and all the distinct zero modes dressings define monopole operators with different quantum numbers but with equal scaling dimensions. In particular, for a minimal magnetic charge $q = 1/2$, there are precisely $\binom{2N_f}{N_f}$ monopole operators [9].

B. Confinement-deconfinement transition to an antiferromagnet

We mentioned in the last section that non-compact QED₃ provides an incomplete IR description of compact QED₃ if monopoles are relevant excitations. In fact, the theory is very different in this case. In pure U(1) compact gauge theory, monopole operators are relevant and condense. This leads to confinement and to the emergence of a mass gap [8; 33]. This effect can be prevented if there are enough massless fermion flavors to screen the monopoles. Indeed, at leading order in $1/N_f$, the monopole scaling dimension is proportional to N_f [9; 34]: The operator becomes irrelevant for a sufficiently large number of massless fermion flavors $2N_f$. Otherwise, the fermions confine. Even if monopoles turn out to be irrelevant and do not destabilize QSL phases in magnets described by emergent QED₃, they may play an important role elsewhere in the phase diagram. In particular, as new fermion interactions are tuned, fermion masses can be generated. In this case, the screening effect by fermions is lost and monopoles are free to proliferate.

For the rest of this section, we examine the aforementioned monopole proliferation subsequent to a fermion mass condensation. We study the deformation of compact QED₃ with a chiral Heisenberg Gross-Neveu (cHGN) interaction with coupling strength h

$$S_{\text{QED}_3 - \text{cHGN}} = \int d^3x \left[-\bar{\Psi} \not{D}_a \Psi - \frac{h^2}{2} (\bar{\Psi} \boldsymbol{\sigma} \Psi)^2 \right] + \dots, \quad (4)$$

where the ellipsis denotes the Maxwell free action and the contribution from monopole operators. Here, $\boldsymbol{\sigma}$ is a Pauli matrix vector acting on a SU(2) subspace of flavors. For definiteness, we introduce right now the language natural for quantum magnets. The SU(2) subspace in question consists of two magnetic spin degrees of freedom $\{\uparrow, \downarrow\}$. The other SU(N_f) subspace consists of valley degrees of freedom, i.e. locations of Dirac point in the Brillouin

zone. QED₃ has the full flavor symmetry SU(2N_f).¹ The cHGN interaction breaks down the global flavor symmetry, SU(2N_f) → SU(2) × SU(N_f). This is broken further to SU(N_f) when a spin-Hall mass $\langle \bar{\Psi} \boldsymbol{\sigma} \Psi \rangle$ is condensed following the tuning of the coupling constant h . The condensate direction spontaneously chosen sets a preferred axis of quantization for the magnetic spin. Monopole operators which then condense have, accordingly, spin quantum numbers. We shall examine this point more thoroughly when we discuss the distinct flavors of monopole operators in Sec. IV.

We just described how an AFM order appears when, following the tuning of a spin-dependent fermion interaction, monopole operators proliferate. This mechanism was described in Ref. [30] in the contexts of Kagome antiferromagnets. It was also considered to describe a transition on the square lattice [18] where a SU(N_f)_{valley} breaking interaction, $\delta \mathcal{L} \sim (\bar{\Psi} \mu_z \boldsymbol{\sigma} \Psi)^2$, is considered instead. This confinement of the DSL on the square lattice has also been studied numerically with quantum Monte Carlo [35]. An extended version of this mechanism involving general fermion bilinears was also considered in Ref. [31].

1. Spin-Hall mass condensation in the 1/N_f expansion

In what follows, we demonstrate, using a 1/N_f expansion, that a spin-Hall mass does condense when a sufficiently strong Gross-Neveu interaction is present. Performing a Hubbard-Stratonovich transformation on the action (4), we obtain

$$S'_{\text{QED}_3 - \text{cHGN}} = \int d^3x \left[-\bar{\Psi} (\not{D}_a + \boldsymbol{\phi} \cdot \boldsymbol{\sigma}) \Psi + \frac{2N_f}{2h^2} \phi^2 \right], \quad (5)$$

where $\boldsymbol{\phi}$ is a three-component auxiliary bosonic field and we rescaled h^2 with the number of fermion flavors 2N_f. The fermions can be integrated to a determinant operator. Tracing out the valley subspace, the effective action becomes

$$S_{\text{eff}} = 2N_f \left(-\frac{1}{2} \log \det (\not{D}_a + \boldsymbol{\phi} \cdot \boldsymbol{\sigma}) + \int d^3x \frac{1}{2h^2} \phi^2 \right), \quad (6)$$

where det is the determinant over the magnetic spin and the Dirac spaces. The saddle point solution for the gauge field is $a_\mu = 0$. We take a homogeneous ansatz for the saddle point value of the bosonic field $\langle \boldsymbol{\phi} \rangle = M \hat{n}$, where

\hat{n} is a unit vector. Eigenstates of the resulting determinant operator are plane waves and are used to obtain the saddle point equation for M in a diagonalized form

$$2M \left(\frac{1}{2h^2} - \int \frac{d^3p}{(2\pi)^3} \frac{1}{p^2 + M^2} \right) = 0. \quad (7)$$

There is a trivial solution $M = 0$ which represents the symmetric phase. A critical coupling h_c^{-2} defines the transition to the ordered phase $M > 0$ through the relation

$$\frac{1}{2h_c^2} = \int \frac{d^3p}{(2\pi)^3} \frac{1}{p^2} = 0, \quad (8)$$

where we used a zeta function regularization to evaluate the divergent integral. For future reference, we evaluate the effective action (6) at the critical point (8)

$$S_{\text{eff}}^c = -N_f \log \det (\not{D}_a + \boldsymbol{\phi} \cdot \boldsymbol{\sigma}). \quad (9)$$

In the ordered phase, the expectation value of the bosonic field can be found by rewriting the saddle point equation as

$$\frac{1}{2h_c^2} - \frac{1}{2h^2} = \int \frac{d^3p}{(2\pi)^3} \left[\frac{1}{p^2} - \frac{1}{p^2 + M^2} \right]. \quad (10)$$

Using (8), we find $M = -2\pi h^{-2}$ for $h^{-2} < 0$. More generally, the condensed mass is given by

$$\langle |\boldsymbol{\phi}| \rangle \equiv M = \begin{cases} 0, & h^{-2} > h_c^{-2}, \\ 2\pi (h_c^{-2} - h^{-2}), & h^{-2} < h_c^{-2}. \end{cases} \quad (11)$$

Note that in momentum regularization we would have obtained a non-zero value for the critical coupling, h_c^{-2} .

III. SCALING DIMENSIONS OF MONOPOLE OPERATORS

We established in Sec. IIB the existence of the large- N_f QED₃–cHGN critical fixed point in the non-compact theory which leads to a spin-Hall mass condensation. In turn, this implies the proliferation of monopoles in the compact theory. Given the primordial role that monopole operators play in the quantum phase transition, we compute their scaling dimensions at the QCP. We shall restrict our computation to leading order in 1/N_f.

Monopole operators are usually defined as operators with the lowest scaling dimension among $4\pi q$ flux-creating operators. In QED₃, there are many monopole operators due to the presence of fermion zero modes [9]. One important result we shall show in the next section is that the analogous operators in QED₃–cHGN develop a non-trivial hierarchy in their scaling dimensions. Nevertheless, we keep referring to those operators as monopole operators. In the present section, we will compute the lowest scaling dimension among these monopole operators.

¹ The center of SU(2N_f) coincides with U(1) gauge transformations and we should quotient the symmetry group [31]. For simplicity, we keep the redundancy and refer to SU(2N_f) as the flavor symmetry group.

A. State-operator correspondence and $1/N_f$ expansion

A monopole operator \mathcal{M}_q^\dagger is characterized by a scaling dimension $\Delta_{\mathcal{M}_q}$ which determines the power law decay of its two-point correlation function. The scaling dimension can be determined through the state-operator correspondence. This correspondence implies that the insertion of a local operator at the origin of flat spacetime $\mathbb{R}^{1,2}$ can be mapped to a state of the conformal field theory (CFT) on $S^2 \times \mathbb{R}$ (see [36] for a clear and concise explanation of this correspondence). Specifically, the monopole operator with the lowest scaling dimension corresponds to the ground state of fermions in QED₃ – cHGN living on S^2 in a background magnetic flux $4\pi q$. The relation also implies that the energy F_q of this ground state and the scaling dimension of this monopole operator $\Delta_q = \min(\Delta_{\mathcal{M}_q})$ are equal

$$\Delta_q = F_q \equiv -\log Z_{S^2 \times \mathbb{R}}[A^q], \quad (12)$$

where A^q is an external gauge field yielding the magnetic flux $\int_{S^2} dA^q = 4\pi q$. The notation F_q stands for free energy, which, in the present non-thermal setup, is the same as the ground state energy.² Our strategy to obtain the scaling dimension Δ_q will be to perform a $1/N_f$ expansion of the free energy

$$F_q = N_f F_q^{(0)} + F_q^{(1)} + \dots \quad (13)$$

We restrict our study to leading order in $1/N_f$ ³

$$\Delta_q^{(0)} = F_q^{(0)}. \quad (14)$$

The state-operator correspondence was first used to compute the scaling dimension of a topological disorder operator in the context of QED₃ [9]. A similar computation was made for the bosonic theory CP^{N_b-1} [38]. The path integral formalism was also used to obtain $1/N$ corrections for QED₃ [39] and CP^{N_b-1} [40]. The ungauged version of CP^{N_b-1} was also investigated using these techniques [41]. Monopole operators were also studied in non-abelian gauge theories, in presence of supersymmetries and in presence of a Chern-Simons term [37; 42–44].

B. Spectrum of the Dirac operator with a spin-Hall mass

In order to obtain the free energy F_q , we study the effective action obtained after integrating out the fermions.

The analysis is similar to the one in Sec. IIB, but we must now work on a sphere with a background magnetic flux. This latter consideration is incorporated through an external gauge field

$$A^q(x) = q(1 - \cos \theta) d\phi, \quad (15)$$

whose flux integral is $\int dA^q = 4\pi q$. The singular part at the south pole $\theta = \pi$ can be compensated by a Dirac string. The requirement that the Dirac string should be invisible imposes the Dirac condition $2q \in \mathbb{Z}$. On the other hand, the spacetime $S^2 \times \mathbb{R}$ is encoded in a non-trivial metric $g_{\mu\nu}(x)$ which we parameterize with (θ, ϕ, τ)

$$g_{\mu\nu} dx^\mu dx^\nu = d\tau^2 + R^2 (d\theta^2 + \sin^2 \theta d\phi^2), \quad (16)$$

where R is the radius of S^2 . The metric can be decomposed as $g_{\mu\nu} = e_\mu^a e_\nu^b \eta_{ab}$, where η_{ab} is the flat spacetime metric and $e_\mu^a(x)$ are the tetrad fields. A spin connection Ω_μ transporting the fermion fields on the curved spacetime can be found from the tetrad fields. Taking into account both U(1) and spacetime connections, the Dirac operator in the critical action (9) now reads [45]

$$\not{D}_{a,A^q}^{S^2 \times \mathbb{R}} = e_b^\mu \gamma^b [\partial_\mu + \Omega_\mu - i(A_\mu^q + a_\mu)] . \quad (17)$$

The critical effective action S_{eff}^c (9) with the modified Dirac operator, $\not{D}_a \rightarrow \not{D}_{a,A^q}^{S^2 \times \mathbb{R}}$, becomes

$$S_{\text{eff}}^c = -N_f \log \det \left(\not{D}_{a,A^q}^{S^2 \times \mathbb{R}} + \phi \cdot \boldsymbol{\sigma} \right). \quad (18)$$

The saddle point condition for this modified effective action still implies a vanishing expectation value for the gauge field $\langle a_\mu \rangle = 0$. We take a homogeneous ansatz for the saddle point value of the bosonic field on the sphere with flux $4\pi q$, $\langle \phi \rangle = M_q \hat{n}$, where \hat{n} is a unit vector. Without loss of generality, we can orient the condensate such that $\hat{n} = \hat{z}$. Inserting this ansatz in the effective action (18), we find the leading order free energy

$$F_q^{(0)} = -\log \det (\not{D}_{A^q} + M_q \sigma_z), \quad (19)$$

where $\not{D}_{A^q} \equiv \not{D}_{a,A^q}^{S^2 \times \mathbb{R}}|_{a=0}$.⁴ The spectrum of the operator appearing inside the determinant in Eq. (19) must be found to obtain the leading order free energy $F_q^{(0)}$.

We first review how the spectrum of the Dirac operator \not{D}_{A^q} was found in Refs. [9; 39] by using analogs of spherical harmonics [46] appropriate for describing spin-1/2 particles in the monopole background. A first step in the generalization is to define the generalized angular momentum $L_q^i = -i\epsilon_{ijk} x_j (\partial_k - A_k^q) - r^2 \epsilon_{ijk} \partial_j A_k^q$ which includes the effect of the magnetic charge. The $SU(2)$

² The free energy should be understood as a zero-temperature limit, $\lim_{\beta \rightarrow \infty} (-\log Z_{S^2 \times S_\beta^1}[A^q]/\beta)$ [37]. This definition is considered when needed later on.

³ The appropriate relation is actually $\Delta_q^{(0)} = F_q^{(0)} - F_{q=0}^{(0)}$, but we find later on that for the case we study, $F_{q=0}^{(0)} = 0$.

⁴ In this section, we simply write \not{D}_{A^q} as we assume a curved spacetime $S^2 \times \mathbb{R}$ whenever the external gauge field A^q is present.

algebra remains after the generalization, $[L_q^i, L_q^j] = i\epsilon_{ijk}L_q^k$, so there exists eigenfunctions $Y_{q,\ell,m}(\theta, \phi)$, called monopole harmonics, which simultaneously diagonalize L_q^2 and L_q^z [46]

$$L_q^2 Y_{q,\ell,m} = \ell(\ell+1) Y_{q,\ell,m}, \quad \ell = |q|, |q|+1, \dots \quad (20)$$

$$L_q^z Y_{q,\ell,m} = m Y_{q,\ell,m}, \quad m = -\ell, -\ell+1, \dots, \ell. \quad (21)$$

As the Dirac operator acts on spinors, one must consider the total angular momentum $\mathbf{J}_q = \mathbf{L}_q + \boldsymbol{\tau}/2$ as well. Two-component spinors $S_{q,\ell,m}^\pm$ that diagonalize the operators $\{L_q^2, J_q^z, J_q^2\}$ are thus introduced

$$J_q^2 S_{q,\ell,m}^\pm = j_\pm(j_\pm+1) S_{q,\ell,m}^\pm, \quad j_\pm = \ell \pm 1/2, \quad (22)$$

$$L_q^2 S_{q,\ell,m}^\pm = \ell(\ell+1) S_{q,\ell,m}^\pm, \quad (23)$$

$$J_q^z S_{q,\ell,m}^\pm = (m+1/2) S_{q,\ell,m}^\pm. \quad (24)$$

Such spinors $S_{q,\ell,m}^\pm$, dubbed spinor monopole harmonics, are built using monopole harmonics as components [9; 39]

$$S_{q,\ell,m}^+ = \begin{pmatrix} \sqrt{\frac{\ell+m+1}{2\ell+1}} Y_{q,\ell,m} \\ \sqrt{\frac{\ell-m}{2\ell+1}} Y_{q,\ell,m+1} \end{pmatrix}, \quad (25)$$

$$S_{q,\ell,m}^- = \begin{pmatrix} -\sqrt{\frac{\ell-m}{2\ell+1}} Y_{q,\ell,m} \\ \sqrt{\frac{\ell+m+1}{2\ell+1}} Y_{q,\ell,m+1} \end{pmatrix}. \quad (26)$$

These spinors can be organized as doublets $[S_{q,\ell-1,m}^+, S_{q,\ell,m}^-]^\top$ with total angular momentum $j = \ell - 1/2$. Adding plane waves $e^{-i\omega\tau}$ to describe the “time” direction⁵, the action of the Dirac operator on this basis is [9; 39]

$$\not{D}_{A^q} \begin{bmatrix} e^{-i\omega\tau} S_{q,\ell-1,m}^+ \\ e^{-i\omega\tau} S_{q,\ell,m}^- \end{bmatrix} = -i\mathbf{O}_{q,\ell}(\omega + i\mathbf{P}_{q,\ell}) \begin{bmatrix} e^{-i\omega\tau} S_{q,\ell-1,m}^+ \\ e^{-i\omega\tau} S_{q,\ell,m}^- \end{bmatrix} \quad (27)$$

where the matrices $\mathbf{O}_{q,\ell}$ and $\mathbf{P}_{q,\ell}$ are given by

$$\mathbf{O}_{q,\ell} = \frac{1}{\ell} \begin{bmatrix} -q & -R\varepsilon_\ell^0 \\ -R\varepsilon_\ell^0 & q \end{bmatrix}, \quad \mathbf{P}_{q,\ell} = \frac{\varepsilon_\ell^0}{\ell} \begin{bmatrix} R\varepsilon_\ell^0 & -q \\ -q & -R\varepsilon_\ell^0 \end{bmatrix} \quad (28)$$

and where $\varepsilon_\ell^0 \equiv R^{-1}\sqrt{\ell^2 - q^2}$. For the minimal total angular momentum $j = |q| - 1/2$, only the spinor $S_{q,|q|,m}^-$ is defined⁶ and the action of the Dirac operator on this

mode reduces to

$$\not{D}_{A^q} \begin{bmatrix} 0 \\ e^{-i\omega\tau} S_{q,|q|,m}^- \end{bmatrix} = -i\omega \operatorname{sgn}(q) \begin{bmatrix} 0 \\ e^{-i\omega\tau} S_{q,|q|,m}^- \end{bmatrix}. \quad (29)$$

This mode has a vanishing energy and thus corresponds to a fermion zero mode in the monopole background.

We now study the complete determinant operator with the contribution of the spin-Hall mass term appearing in Eq. (19). The additional term is diagonal in the spinor monopole harmonics basis. Therefore, we can still use this basis to compute the determinant operator

$$\begin{aligned} \log \det (\not{D}_{A^q} + M_q \sigma_z) &= \sum_{\sigma=\pm 1} \int_{-\infty}^{\infty} \frac{d\omega}{2\pi} \\ &\times \left[d_{|q|} \log [-i\omega \operatorname{sgn}(q) + M_q \sigma] \right. \\ &+ \left. \sum_{\ell=|q|+1}^{\infty} d_\ell \log \det [-i\mathbf{O}_{q,\ell}(\omega + i\mathbf{P}_{q,\ell}) + M_q \sigma] \right], \quad (30) \end{aligned}$$

where $d_\ell = 2\ell$ is the degeneracy coming from azimuthal quantum numbers. Simplifying further, we obtain

$$\begin{aligned} \log \det (\not{D}_{A^q} + M_q \sigma_z) &= \sum_{\sigma=\pm 1} \int_{-\infty}^{\infty} \frac{d\omega}{2\pi} \\ &\times \left[d_{|q|} \log [\omega + iM_q \sigma \operatorname{sgn}(q)] \right. \\ &+ \left. \sum_{\ell=|q|+1}^{\infty} d_\ell \log [\omega^2 + (\varepsilon_\ell^0)^2 + M_q^2] \right] \\ &= \int_{-\infty}^{\infty} \frac{d\omega}{2\pi} \left[d_{|q|} \log (\omega^2 + M_q^2) + \sum_{\ell=|q|+1}^{\infty} 2d_\ell \log [\omega^2 + \varepsilon_\ell^2] \right], \quad (31) \end{aligned}$$

where we removed inessential constants and we defined the mass-deformed eigenvalues

$$\varepsilon_\ell = R^{-1} \sqrt{\ell^2 - q^2 + M_q^2 R^2}. \quad (32)$$

We now explicitly write the spectrum of the Dirac operator with a spin-Hall mass on the magnetically charged sphere found from (30)

$$\omega + i\sigma \operatorname{sgn}(q) \varepsilon_{|q|}, \quad \ell = |q|, \quad (33)$$

$$\pm \sqrt{\omega^2 + \varepsilon_\ell^2}, \quad \ell = \{|q|+1, |q|+2, \dots\}, \quad (34)$$

where $\sigma \in \{-1, +1\}$. The \pm modes for $\ell \geq |q|+1$ in (34) are referred to as conduction (+) and valence (−) modes. There is no such doubling of the $\ell = |q|$ modes in (33) which are descendants of the QED₃ zero modes. This is why we refer to these modes as “zero” modes even though they have non-vanishing energy $\pm \varepsilon_{|q|} = \pm M_q$ with the

⁵ We emphasize that this “time” dimension on $S^2 \times \mathbb{R}$ does not correspond to the original time dimension on $\mathbb{R}^{1,2}$.

⁶ The other would-be spinor $S_{q,|q|-1,m}^+$ with $j = |q| - 1/2$ does not exist since $\ell = |q| - 1$ is smaller than the minimal angular momentum allowed for monopole harmonics (20).

inclusion of the spin-Hall mass. We restate that the σ eigenvalue refers to magnetic spin orientation relative to the quantization axis defined by $\langle \phi \rangle$. For positive magnetic charge $q > 0$, a “zero” mode with spin up, $\sigma = 1$, has an energy $\varepsilon_{|q|} = M_q$, whereas a spin down “zero” mode, $\sigma = -1$ has an opposite energy $-M_q$. These “zero” modes are responsible for the first term in Eq. (31)

C. Scaling dimension computation

The free energy at leading order (19) is rewritten using the result (31) (from now on, we assume a positive magnetic charge $q > 0$),

$$F_q^{(0)} = - \int \frac{d\omega}{2\pi} \left[d_q \log [\omega^2 + M_q^2] + \sum_{\ell=q+1}^{\infty} 2d_\ell \log [\omega^2 + \varepsilon_\ell^2] \right], \quad (35)$$

where the radius R of the sphere was eliminated by changing the integration variable $\omega \rightarrow \omega/R$, by rescaling the parameters $\{\varepsilon_\ell, F_q^{(0)}, M_q\} \rightarrow \{\varepsilon_\ell, F_q^{(0)}, M_q\}/R$ and by removing an inessential constant. The free energy (35) needs regularization. We first treat the diverging integral over frequencies by rewriting the integrand using the identity $\log A = -dA^{-s}/ds|_{s=0}$ and doing an analytic continuation to $s = 0$. This procedure is presented in App. A. The resulting free energy is

$$F_q^{(0)} = -d_q M_q - \sum_{\ell=q+1}^{\infty} 2d_\ell \varepsilon_\ell. \quad (36)$$

By setting $M_q = 0$ in this free energy, we obtain the QED₃ results shown in Ref. [39].⁷ This free energy (36) still needs regularization. The divergent sum is rewritten by adding and subtracting its diverging part

$$\begin{aligned} \sum_{\ell=q+1}^{\infty} d_\ell \varepsilon_\ell &= \sum_{\ell=q+1}^{\infty} \left[2\ell \sqrt{\ell^2 + M_q^2 - q^2} - 2\ell^2 - (M_q^2 - q^2) \right] \\ &+ 2 \sum_{\ell=q+1}^{\infty} \left[\ell^{2(1-s)} + \left(\frac{1}{2} - s \right) (M_q^2 - q^2) \ell^{-2s} \right] \Big|_{s=0}. \end{aligned} \quad (37)$$

Now, only the last sum is divergent and we treat it with a zeta function regularization by using $\sum_{n=0}^{\infty} (n+a)^{-s} = \zeta(s, a)$. This sum then becomes $2\zeta(-2, q+1) + (M_q^2 - q^2) \zeta(0, q+1)$, an expression for which a polynomial form may be found using Ref. [47].

The resulting finite expression is then inserted in (36) to obtain the regularized free energy

$$F_q^{(0)} = -d_q M_q - \sum_{\ell=q+1}^{\infty} \left[2d_\ell \varepsilon_\ell - d_\ell^2 - 2(M_q^2 - q^2) \right] + (2q+1)(M_q^2 - q(q-2)/3). \quad (38)$$

We can then find the regularized gap equation, i.e. the saddle-point equation $\partial F_q^{(0)}/\partial M_q = 0$

$$-d_q + 2M_q(2q+1) - 2M_q \sum_{\ell=q+1}^{\infty} [d_\ell \varepsilon_\ell^{-1} - 2] = 0. \quad (39)$$

For a vanishing magnetic charge $q = 0$, the contribution from “zero” modes vanishes since $d_{q=0} = 0$. The saddle point equation then only has a trivial solution $M_{q=0} = 0$. This case coincides with QED₃ where there is no mass M_q to start with and the free energy vanishes, $F_{q=0}^{(0)} = 0$. For $q \neq 0$, the saddle point equation only has a non-trivial solution $M_q > 0$ which must be determined numerically.⁸ The resulting mass M_q is then inserted in (38) to obtain the scaling dimension at leading order in $1/N_f$, $\Delta_q = N_f F_q^{(0)} + \mathcal{O}(N_f^0)$. The mass M_q and the scaling dimension of monopole operators in QED₃ - cHGN and QED₃ are obtained for multiple values of q and are shown in Tab. I. These numerical results are also plotted

Table I: Numerical results for the mass M_q and the lowest scaling dimension of monopole operators in QED₃ - cHGN and QED₃, respectively Δ_q and $\Delta_q^{\text{QED}_3} = \Delta_q|_{M_q=0}$. These results are at leading order in $1/N_f$. We show the scaling dimensions per number of fermion flavors $2N_f$. These quantities are shown for the first few allowed values of the magnetic charge q .

q	M_q	$\frac{1}{2N_f} \Delta_q$	$\frac{1}{2N_f} \Delta_q^{\text{QED}_3}$
0	0	0	0
0.5	0.27318	0.19539	0.26510
1.0	0.41395	0.46039	0.67315
1.5	0.51946	0.78471	1.18643
2.0	0.60728	1.15964	1.78690
2.5	0.68406	1.57928	2.46345
3.0	0.75311	2.03939	3.20837
3.5	0.81638	2.53671	4.01591
4.0	0.87510	3.06867	4.88154
4.5	0.93014	3.63315	5.80162
5.0	0.98211	4.22839	6.77309

in Fig. 1 and Fig. 2 along with corresponding analytical approximations obtained in Sec. III D. The numerical

⁷ Our definition of $F_q^{(0)}$ has an extra factor of 2 because we defined the total number of fermion flavors as $2N_f$ but we expanded the free energy in powers of $1/N_f$ (13). This procedure is more natural since the spin degeneracy does not factor out like the valley degeneracy because of the “zero” modes.

⁸ If the “time” direction \mathbb{R} is compactified on a circle S^1_β , a trivial solution does exist for $q > 0$. It persists as the radius β is taken to infinity to retrieve the real line. However, this solution is a *maximum* of free energy and does not determine Δ_q . See App. B

and analytical results agree very well even for small values of q . We also note that the monopole operator scaling dimension is always smaller in $\text{QED}_3 - \text{cHGN}$ than in QED_3 . The fact that $\Delta_q \leq \Delta_q^{\text{QED}_3}$ is expected since the case $M_q = 0$ implies $\Delta_q = \Delta_q^{\text{QED}_3}$ and sets an upper bound for the scaling dimension Δ_q . Setting $2N_f = 4$

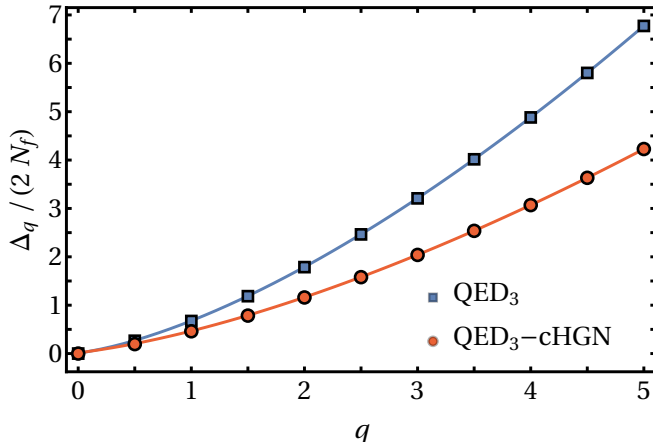


Figure 1: Lowest scaling dimension of monopole operators Δ_q per number of fermion flavors $2N_f$ as a function of the magnetic charge q . Analytical approximations in the large q limit of the scaling dimension in $\text{QED}_3 - \text{cHGN}$ and QED_3 , respectively (50) and (51), are plotted in solid lines. These are compared to their respective numerical values shown in Tab. I.

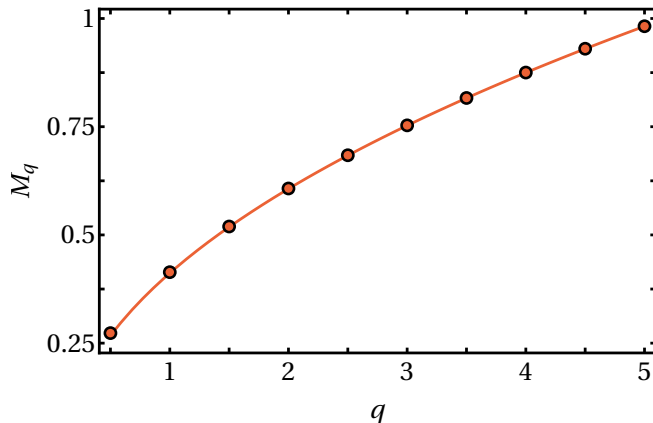


Figure 2: Mass $M_q \equiv \langle |\phi| \rangle$ as a function of the magnetic charge q at leading order in $1/N_f$. The solid line corresponds to the large q analytical approximation of M_q (48). The circles are the numerical values of M_q shown in Tab. I.

gives an estimate on the scaling dimension of monopole operators for certain quantum magnets. One should be careful with these results as the expansion parameter is not small and corrections to the leading order may be important. Nevertheless, if we consider the monopole operator with a minimal magnetic charge $q = 1/2$, the

lowest scaling dimension is

$$\Delta_{q=1/2} = 2N_f \cdot 0.19539 + \mathcal{O}(N_f^0). \quad (40)$$

In the case $2N_f = 4$, which is interesting for application to quantum magnets, we find a strongly relevant operator

$$\Delta_{q=1/2} \Big|_{2N_f=4} \approx 0.78156 < 3. \quad (41)$$

However, the monopole operator with the minimal magnetic charge is not allowed in many contexts, we discuss this matter in Sec. VII. We also note that the unitarity bound is violated for $2N_f < 2.56$ as $\Delta_{q=1/2} < 1/2$ [36]. It would be interesting to see if the violation persists with higher order corrections. This would shed light on the phase diagram of QED_3 at $2N_f = 2$.

For demonstration purpose, we plot in Fig. 3 the free energy for the minimal magnetic charge as a function of the mass $M_{q=1/2}$. The free energy minimum is identified and corresponds to the solution to the saddle point equation, $M_{q=1/2} = 0.27318$, as shown in Tab. I. For large values of $M_{q=1/2}$, the sum in (38) can be approximated as an integral, and we find that the free energy grows as $F_{q=1/2}^{(0)} \sim 4(M_{q=1/2})^3/3$ at leading order in $M_{q=1/2}$.

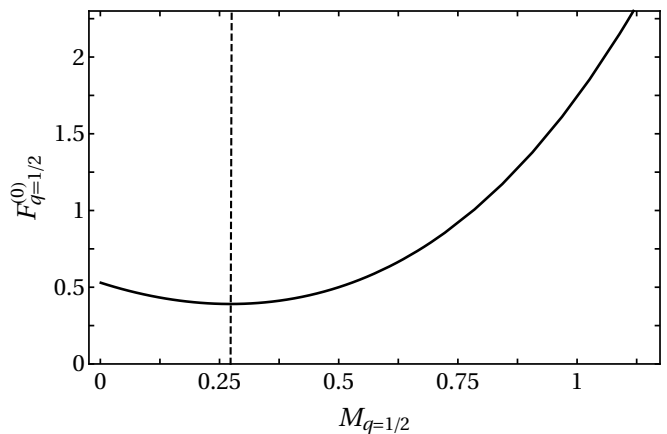


Figure 3: Leading order in $1/N_f$ of the free energy with minimal magnetic charge $F_{q=1/2}^{(0)}$ (38) as a function of the mass $M_{q=1/2}$. The appropriate value of the mass $M_{q=1/2}$ found with the saddle point equation (39) corresponds to the minimum of this function. For large mass, the free energy behaves as $F_{q=1/2}^{(0)} \sim 4(M_{q=1/2})^3/3$.

Let us restate one important result. For $q \neq 0$, we found that the monopole operator with the lowest scaling dimension is described with a mass condensate, $M_q \equiv \langle |\phi| \rangle > 0$. We stress out that this does not imply a non-vanishing spin-Hall mass expectation value at the critical point of the phase transition. Our computation is done on a compact space using the state-operator correspondence and simply serves as way to compute the scaling dimension. The condensate is natural in this context since, once R is reintroduced by undoing our previous

rescaling (35), there is a characteristic length to build a non-vanishing mass $M_q \propto R^{-1}$.

D. Monopole scaling dimensions for large q

We now obtain an analytical approximation of the condensed mass M_q and the lowest scaling dimension of monopole operators Δ_q by studying the free energy $F_q^{(0)}$ in a large q limit. It is simpler to work with the unregularized free energy (36). We first change the summation index $\ell \rightarrow \ell + q + 1$ so that only the summand depends on q . The free energy then becomes

$$F_q^{(0)} = -2qM_q - 4 \sum_{\ell=0}^{\infty} (\ell + q + 1) \sqrt{(\ell + q + 1)^2 - q^2 + M_q^2}. \quad (42)$$

The saddle point equation $\partial F_q^{(0)} / \partial M_q = 0$ defining the mass M_q is, up to multiplicative factors,

$$q + 2M_q \sum_{\ell=0}^{\infty} \frac{\ell + q + 1}{\sqrt{(\ell + q + 1)^2 + M_q^2 - q^2}} = 0. \quad (43)$$

We introduce an ansatz for the mass squared that is inspired by an analog computation in the bosonic theory CP^{N-1} [40]

$$M_q^2 = 2\chi_0 q + \chi_1 + \mathcal{O}(q^{-1}). \quad (44)$$

With this ansatz, we expand Eq. (43) in powers of $1/q$. Using once again the zeta function regularization, the condition becomes

$$0 = 4q^{1/2} \left(2\zeta_{1/2} + \chi_0^{-1/2} \right) - q^{-1/2} \left(2(\chi_1 + \chi_0^2) \zeta_{3/2} + 4\chi_0 \zeta_{1/2} - 6\zeta_{-1/2} + \chi_1 \chi_0^{-3/2} \right) + \mathcal{O}(q^{-3/2}), \quad (45)$$

where we defined $\zeta_s \equiv \zeta(s, 1 + \chi_0)$.⁹ Solving (45) order by order, we find a transcendental condition defining χ_0 and a linear condition for χ_1

$$2\zeta_{1/2} + \chi_0^{-1/2} = 0, \quad (46)$$

$$\chi_1 + \frac{2\chi_0^{3/2} (\chi_0^2 \zeta_{3/2} + 2\chi_0 \zeta_{1/2} - 3\zeta_{-1/2})}{1 + 2\chi_0^{3/2} \zeta_{3/2}} = 0. \quad (47)$$

Inserting the solution of (46, 47) into the mass ansatz (44), we find the mass squared $M_q^2 = 0.199q - 0.030 + \mathcal{O}(q^{-1})$ from which the mass is found to be

$$M_q = 0.446q^{1/2} - 0.0341q^{-1/2} + \mathcal{O}(q^{-3/2}). \quad (48)$$

As shown in Fig. 2, this asymptotic expansion is found to agree extremely well with the exact mass M_q , even at small magnetic charge q .

We repeat this procedure for the free energy. We insert the mass ansatz (44) in the free energy (42) and we perform a $1/q$ expansion

$$\begin{aligned} \frac{1}{2} F_q^{(0)} = & -\sqrt{2}q^{3/2} \left(2\zeta_{-1/2} + \chi_0^{1/2} \right) - \frac{q^{1/2}}{\sqrt{2}} \left((\chi_0^2 + \chi_1) \zeta_{1/2} \right. \\ & \left. - 6\chi_0 \zeta_{-1/2} + 5\zeta_{-3/2} + \frac{1}{2} \chi_1 \chi_0^{-1/2} \right) + \mathcal{O}(q^{-1/2}). \end{aligned} \quad (49)$$

Inserting the solution of (46, 47) in this result, we obtain the leading order scaling dimension (14)

$$\Delta_q = 2N_f \left(0.356q^{3/2} + 0.111q^{1/2} + \mathcal{O}(q^{-1/2}) \right) + \mathcal{O}(N_f^0). \quad (50)$$

The scaling dimension for QED₃ is found by doing the same expansion but starting with $M_q = 0$

$$\Delta_q^{\text{QED}_3} = 2N_f \left(0.588q^{3/2} + 0.090q^{1/2} + \mathcal{O}(q^{-1/2}) \right) + \mathcal{O}(N_f^0). \quad (51)$$

Once again, these asymptotic expansions are in good agreement with the corresponding numerical results as shown in Fig. 1. Note that there is no term at order q^0 in the scaling dimensions at leading order in $1/N_f$ (50, 51). This is expected since all CFTs in $d = 2 + 1$ dimensions with a U(1) global charge should have the same q^0 term [48; 49]. As such, it can't depend on N_f . It thus has to vanish at order N_f .

We take a step back to appreciate the leading order relation $\Delta_q^{(0)} \sim q^{3/2}$. We recall that the theory is set on $S^2 \times \mathbb{R}$. The background magnetic flux on the sphere is $BR^2 = q$, where B is the magnetic field and R is the radius of the sphere. Taking $q \rightarrow \infty$ and $R \rightarrow \infty$ while keeping B finite, the theory is reduced to Dirac fermions on a plane in a uniform magnetic field. The eigenvalues are then given by relativistic Landau levels

$$E_n = \sqrt{2B(n + 1/2) + M_q^2} \approx R^{-1}q^{1/2} \sqrt{2(n + 1/2) + 2\chi_0}. \quad (52)$$

In terms of a free energy density $[\mathcal{F}_q] = [E]^3$, this means we have $\mathcal{F}_q \sim R^{-3}q^{3/2}$. The free energy should then scale as $F_q^{(0)} \sim R^2 \mathcal{F}_q \sim R^{-1}q^{3/2}$. Reintroducing a missing power of R in (49) that was rescaled away in (35), this is indeed the relation we get. The behaviour $\Delta_q^{(0)} \sim q^{3/2}$ is then coherent with the large- q interpretation in terms of Landau levels.

IV. MONOPOLE DRESSING

In the previous section where we computed the lowest scaling dimension of monopole operators Δ_q , the

⁹ Neglecting powers of ℓ compared to powers of q in the large- ℓ portion of the sum in condition (43) may seem problematic. These terms do appear to higher order in $1/q$ but cause no problem once properly regularized.

fermionic occupation of the corresponding ground state was not explicated. In this section, we specify the “zero” modes dressing of this ground state and consider other possible “zero” modes dressings defining other monopole operators. We show a non-trivial hierarchy in the scaling dimensions of monopole operators in $\text{QED}_3 - \text{cHGN}$ that is not present in QED_3 .

Monopole operators correspond to $U(1)$ gauge invariant states which means they have a vanishing fermion number $\langle \hat{N} \rangle$. In a \mathcal{CT} quantized theory where $\{CT, \hat{N}\} = 0$, this condition enforces half filling of the fermion modes. The monopole operators correspond to states where the Dirac sea is filled as well as half of the “zero” modes. This condition that was discussed in the case of QED_3 [9]. It is also valid in $\text{QED}_3 - \text{cHGN}$ where the spectrum has the same structure, as was shown in Sec. III. One other consideration is that monopole operators should be Lorentz scalars. We shall focus on $q = 1/2$ monopoles where this is not an issue as the unique “zero” mode for each fermion flavor corresponds to a $j = 0$ Lorentz $SU(2)_{\text{rot}}$ singlet [9].

The energy spectrum of fermions in the monopole background (33, 34) shows that spin down “zero” modes have a lower energy than spin up “zero” modes. The monopole operator with the lowest scaling dimension Δ_q thus corresponds to the state with all the spin down “zero” modes occupied and all the spin up “zero” modes empty, as shown in Fig. 4. We refer to this operator as the ground state monopole. This fermionic configuration

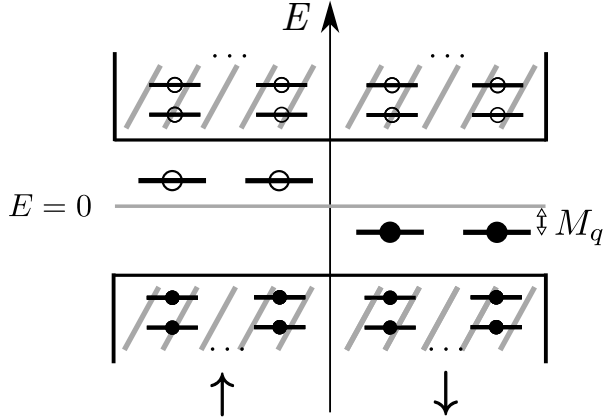


Figure 4: Schematic representation of the energy spectrum and fermionic occupation for the ground state monopole in presence of a spin-Hall mass $M_q \sigma^z$. The spectrum is shown for $2N_f = 4$ fermion flavors and minimal magnetic charge $q = 1/2$. Modes with spin up (down) are shown on left (right). A state of minimal energy is achieved by occupying all the Dirac sea as well as all the spin down zero modes which have energy $-M_q$.

can also be read off the free energy (36) by rewriting it

suggestively as

$$F_q^{(0)} = d_q(-M_q) \left(\frac{1}{2} \right) + d_q(M_q) \left(-\frac{1}{2} \right) + \sum_{\ell=q+1}^{\infty} \left[2d_\ell(-\varepsilon_\ell) \left(\frac{1}{2} \right) + 2d_\ell(\varepsilon_\ell) \left(-\frac{1}{2} \right) \right]. \quad (53)$$

This form puts emphasis on the fact that modes with positive (negative) energy are empty (filled), corresponding to an occupation factor $\langle c_n^\dagger c_n - 1/2 \rangle = \mp 1/2$, where c_n^\dagger are the creation operators for the fermion modes in the monopole background.

We now evaluate the scaling dimensions of monopole operators, which are defined by the various “zero” modes dressings. These operators can be built by annihilating some or all the spin down “zero” modes of the ground state monopole and creating an equal amount of spin up “zero” modes. Each such change increases the energy by $M_q - (-M_q) = 2M_q$. We study explicitly excited monopole operators with minimal magnetic charge $q = 1/2$. For example, the first excited monopole operator, whose fermionic occupation is represented in Fig. 5(a), has a scaling dimension $\Delta_{q=1/2}^+ = \Delta_{q=1/2} + 2M_{q=1/2}$. The monopole operator dressed with all the N_f spin up “zero” modes, represented in Fig. 5(b), has the largest scaling dimension among monopole operators which is $\Delta_{q=1/2}^\uparrow = \Delta_{q=1/2} + 2N_f M_{q=1/2}$. Using

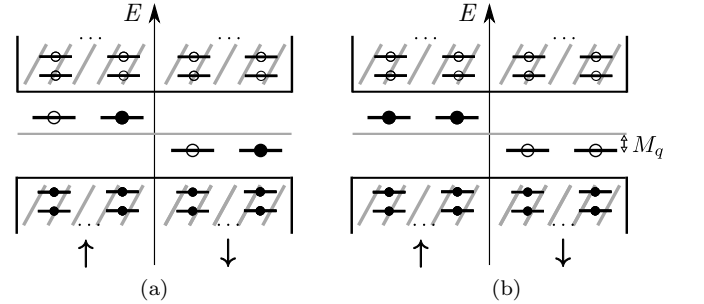


Figure 5: Schematic representation of the fermionic occupation of two excited monopole operators in presence of a spin-Hall mass $M_q \sigma^z$. Modes with spin up (down) are shown on left (right). The spectrum is shown for $2N_f = 4$ fermion flavors and minimal magnetic charge $q = 1/2$. a) First excited monopole operator; b) Monopole operator dressed only with spin up “zero” modes.

the numerical results for the mass $M_{q=1/2}$ in Tab. I, we find leading order scaling dimensions of excited monopole operators

$$\Delta_{q=1/2}^+ - \Delta_{q=1/2} \approx 0.546 + \mathcal{O}(N_f^{-1}), \quad (54)$$

$$\Delta_{q=1/2}^\uparrow - \Delta_{q=1/2} \approx 2N_f(0.273) + \mathcal{O}(N_f^0). \quad (55)$$

The first excited monopole scaling dimension is order $(1/N_f)^0$ larger than the ground state. This difference becomes relatively less important as N_f becomes large. On

the other hand, the scaling dimension of the monopole operator dressed with all spin up “zero” modes is order N_f and the difference with the lowest scaling dimension grows larger as N_f is increased.

We can also find the range of the scaling dimensions analytically for large q . We consider the scaling dimension of the monopole operator dressed with all the $2N_f q$ spin up “zero” modes

$$\Delta_q^\uparrow = \Delta_q + 4N_f q M_q. \quad (56)$$

Using large q results (48, 50), we find the leading order results in $1/N_f$

$$\Delta_q^\uparrow = 2N_f \left(1.248q^{3/2} + 0.0426q^{1/2} + \mathcal{O}(q^{-1/2}) \right) + \mathcal{O}(N_f^0). \quad (57)$$

The hierarchy observed in the scaling dimensions of monopole operators in $\text{QED}_3 - \text{cHGN}$ represents a symmetry lifting of the degenerate monopole multiplet in compact QED_3 . The global $\text{SU}(2N_f)$ flavor symmetry of QED_3 implies that monopole operators are organized in a completely antisymmetric representation of $\text{SU}(2N_f)$ and consequently must have equal scaling dimensions [9]. Indeed, the symmetry is responsible for the degeneracy of the distinct zero modes dressings defining the monopole operators. When the spin-dependent interaction is added, the global symmetry is broken down $\text{SU}(2N_f) \rightarrow \text{SU}(2)_{\text{spin}} \times \text{SU}(N_f)_{\text{valley}}$, and there is a symmetry lifting. This lifting is only partial since, for example, monopole operators with trivial spin quantum numbers remain degenerate, having the same scaling dimensions.

V. COMPARISON WITH $\text{SU}(2N_f)$ SYMMETRIC CRITICAL POINT

Other Gross-Neveu deformations of QED_3 yield distinct CFTs and different monopole operators. In this section, we study the monopole operators at the QCP between a DSL and a chiral spin liquid. In the latter phase, the fermions acquire the same mass, leading to a Chern-Simons term for the dynamical gauge field. This phase transition is driven by the interaction $(\bar{\Psi}\Psi)^2$,

$$S_{\text{QED}_3 - \text{GN}} = \int d^3x \left[-\bar{\Psi} \not{D}_a \Psi - \frac{h^2}{2} (\bar{\Psi}\Psi)^2 \right], \quad (58)$$

where a $\text{SU}(2N_f)$ symmetric mass is condensed for sufficiently strong coupling strength $h > h_c$.

The procedure to obtain the scaling dimensions of monopole operators must be modified. For this model, there is only a single pseudo-scalar boson ϕ entering the Hubbard-Stratonovich transform. The effective action at the critical point can be obtained in the same way we derived the analogous quantity for the spin-dependent case (18)

$$S_{\text{eff}}''^c = -N_f \log \det \left(\not{D}_{a,A^q}^{S^2 \times \mathbb{R}} + \phi \right), \quad (59)$$

where we now work on $S^2 \times \mathbb{R}$ with the sphere pierced by a $4\pi q$ flux. Here, there is no constraint on the sign of the mass given by the expectation value of the bosonic field $M_q = \langle \phi \rangle$.

Another important difference when computing the lowest scaling dimension of monopole operators in this model is that a chemical potential μ must be introduced. This is used to enforce half-filling of the “zero” modes.¹⁰ This was not necessary for the model with a spin-dependent interaction. The reason is that the chemical potential is by default set to zero. Thus, half of the “zero” modes are below this level and get filled up. In QED_3 [9; 39], the zero modes are also half filled as a chemical potential set to zero sits at the level of all the zero modes. This is not the case when a $\text{SU}(2N_f)$ symmetric interaction is activated since the “zero” modes all get shifted below the chemical potential if the boson condensate is non-zero. Thus, directly setting $\mu = 0$ only yields the correct fermionic occupation when there is an equal number of modes above and below zero energy.

The chemical potential can be incorporated within the path integral formalism. We first compactify the “time” direction to a circle S_β^1 with a radius β . This radius is taken to infinity, $\beta \rightarrow \infty$, at the end of our computations. When working on this “thermal” circle, the modified relation between the monopole operator scaling dimension Δ_q and the free energy F_q for $\beta \gg 1$ is [44]

$$\Delta_q - \frac{1}{\beta} \log(\Omega_q) + \mathcal{O}(e^{-c\beta}) = F_q \equiv -\frac{1}{\beta} \log Z_{S^2 \times S_\beta^1}[A^q], \quad (60)$$

where Ω_q is the ground state degeneracy and c gives the energy spacing between the ground state and the first excited state.¹¹ On this space, the chemical potential can be defined as the homogeneous saddle point value of the imaginary gauge field $\langle a_\tau \rangle = -i\mu$. This approach was used in Ref. [44]. The chemical potential is a source for the fermion number $\Psi^\dagger \Psi$. Requiring a vanishing fermion number, we have the condition

$$\frac{1}{\beta} \frac{\delta \ln Z_{S^2 \times S_\beta^1}[A^q]}{\delta \mu} = \langle N_{\text{fermions}} \rangle = 0. \quad (61)$$

This can also be written in terms of a saddle point equation. Once again, the spatial part of the gauge field has a vanishing expectation value $\langle a_i \rangle = 0$. We are left with

¹⁰ We will find that these modes have vanishing energy and are truly zero modes. However, it is simpler for the discussion that follows to assume that these modes might have non-zero energy, so we refer to them as “zero” modes at this point of the analysis.

¹¹ The identity operator ($q = 0$) should have a vanishing scaling dimension $\Delta_{q=0} = 0$ and no degeneracy, $\Omega_{q=0} = 1$. This can be guaranteed by a proper normalization, but just as in the spin-dependent case, it turns out to be unnecessary.

our homogeneous ansatz $\langle a_\tau \rangle = -i\mu$ and $\langle \phi \rangle = M_q$,

$$\frac{\partial F_q^{(0)}}{\partial \mu} = 0, \quad (62)$$

$$\frac{\partial F_q^{(0)}}{\partial M_q} = 0, \quad (63)$$

where the leading order in $1/N_f$ of the free energy is

$$F_q^{(0)} = -\log \det \left(\not{D}_{-i\mu, A^q}^{S^2 \times S_\beta^1} + M_q \right). \quad (64)$$

As the “time” direction is compact, the spectrum of the Dirac operator in Eq. (64) is now defined by Matsubara fermionic frequencies $\omega_n = (2\pi/\beta)(n + 1/2)$ where $n \in \mathbb{Z}$. In contrast to our previous computations, the mass term is now spin symmetric in contrast to our previous computation. With these considerations, the previous result shown in Eq. (31) can be adapted so that (64) becomes

$$F_q^{(0)} = -\frac{2}{\beta} \sum_{n=-\infty}^{\infty} \left[d_q \log [\omega_n - i\mu + iM_q] + \sum_{\ell=q+1}^{\infty} d_\ell \log [(\omega_n - i\mu)^2 + \varepsilon_\ell^2] \right], \quad (65)$$

where as before ε_ℓ is given by Eq. (32). Regularizing the sum over Matsubara frequencies, we obtain

$$F_q^{(0)} = -\frac{2}{\beta} \left[d_q \log \left[2 \cosh \left(\frac{\beta(\mu - M_q)}{2} \right) \right] + \sum_{\ell=q+1}^{\infty} d_\ell \log [2(\cosh(\beta\varepsilon_\ell) + \cosh(\beta\mu))] \right]. \quad (66)$$

The saddle point equations (62, 63) become

$$-d_q \tanh \left(\frac{\beta(\mu - M_q)}{2} \right) - \sum_{\ell=q+1}^{\infty} \frac{2d_\ell \sinh(\beta\mu)}{\cosh(\beta\varepsilon_\ell) + \cosh(\beta\mu)} = 0, \quad (67)$$

$$d_q \tanh \left(\frac{\beta(\mu - M_q)}{2} \right) - \sum_{\ell=q+1}^{\infty} \frac{2d_\ell \varepsilon_\ell^{-1} M_q \sinh(\beta\varepsilon_\ell)}{\cosh(\beta\varepsilon_\ell) + \cosh(\beta\mu)} = 0. \quad (68)$$

Taking $\mu = M_q$ eliminates the first term in both equations. These equations can be further simplified by taking the large β limit. The sum in the first equation vanishes to leading order in $1/\beta$ and the first saddle point equation is then satisfied for $\beta \rightarrow \infty$. In the same way, the second saddle point equation to leading order in $1/\beta$ with $\mu = M_q$ is given by

$$2M_q \sum_{\ell=q+1}^{\infty} d_\ell \varepsilon_\ell^{-1} = 0. \quad (69)$$

In this limit, this saddle point equation is only satisfied for $M_q = 0$, which implies a vanishing chemical potential $\mu = 0$. More directly, this means that the expectation value of the bosonic field vanishes, $\langle \phi \rangle = 0$. Thus, monopole operators at the symmetric QCP are dressed with true zero modes. One of the monopole ground states is shown in Fig. 6. Since there is no boson condensate,

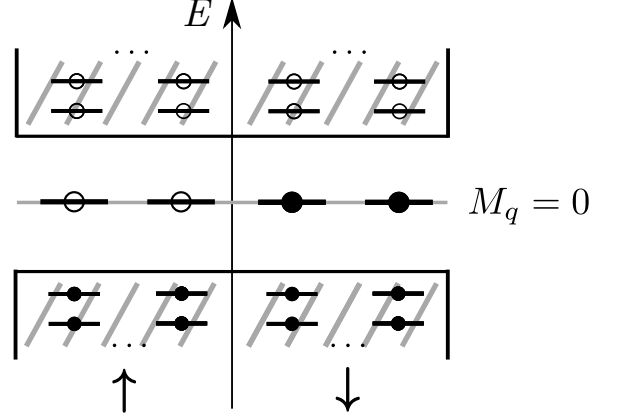


Figure 6: Schematic representation of the energy spectrum and fermionic occupation for one of the monopole ground states in the $SU(2N_f)$ symmetric QCP. The spectrum is shown for $2N_f = 4$ fermion flavors and minimal magnetic charge $q = 1/2$. The zero modes could be shifted by an energy M_q , but the saddle point equations force this quantity to vanish.

the fermion energies are unchanged when compared to those in QED_3 . This means that we are left, at leading order in $1/N_f$, with the same scaling dimensions as in QED_3 , $\Delta_q^{\text{QED}_3 - \text{GN}} = \Delta_q^{\text{QED}_3} + O(1/N_f^0)$. A similar result was obtained for the QCP between a DSL and a \mathbb{Z}_2 -spin liquid [50].

We emphasize that this is a result at leading order in $1/N_f$. The presence of the bosonic field includes more quantum fluctuations that may change corrections at non-leading orders. We also note that the first condition $\mu = M_q$ is indeed the condition enforcing half-filling of the zero modes and is needed even if in the end, we find $\mu = M_q = 0$. Had we not included the chemical potential, we would minimize the free energy that has all the zero modes empty and we would find $M_q \neq 0$. In the case of the spin-dependent interaction we studied before, the saddle point solution for the chemical potential is $\mu = 0$, independently of the value of the mass M_q . We show this explicitly in App. B. This is why the inclusion of a chemical potential was not necessary in this case.

A. Testing a duality with bosonic CP^1 model

The case of compact $\text{QED}_3 - \text{GN}$ theory with $2N_f = 2$ fermion flavors is of particular interest since it is conjectured to be dual to the CP^1 theory when both theories are tuned at their critical point, assuming the fixed

points exist [21]. This latter theory describes $N_b = 2$ flavors of complex bosonic fields forming a $SU(2)$ doublet $z = (z_1, z_2)^T$ which satisfy a length constraint $z^\dagger z = 1$ and interact with a compact gauge field. This model notably describes a deconfined quantum critical point between Néel and VBS phases, which is relevant for quantum magnets on various lattices [51], with the case of square lattice being the prototype example of deconfined criticality [20]. Operators on one side of the conjectured duality have the same scaling dimension as their dual on the other side of the duality. More specifically, the duality relates a set of operators in the fermionic theory

$$\left[\text{Re} \left(\psi_1^\dagger \widetilde{\mathcal{M}}_{q=1/2} \right), -\text{Im} \left(\psi_1^\dagger \widetilde{\mathcal{M}}_{q=1/2} \right), \right. \\ \left. \text{Re} \left(\psi_2^\dagger \widetilde{\mathcal{M}}_{q=1/2} \right), \text{Im} \left(\psi_2^\dagger \widetilde{\mathcal{M}}_{q=1/2} \right), \phi \right], \quad (70)$$

to a set of operators in the bosonic theory

$$\left[2 \text{Re} \mathcal{M}_{q=1/2}^{\text{CP}^1}, 2 \text{Im} \mathcal{M}_{q=1/2}^{\text{CP}^1}, z^\dagger \sigma_1 z, z^\dagger \sigma_2 z, z^\dagger \sigma_3 z \right]. \quad (71)$$

Here, $\psi_{I=1,2}^\dagger \widetilde{\mathcal{M}}_{q=1/2}$ is a monopole with a minimal magnetic charge $q = 1/2$ dressed with one of the two fermion zero modes. On the bosonic side, $\mathcal{M}_{q=1/2}^{\text{CP}^1}$ is the unique monopole operator with a minimal magnetic charge $q = 1/2$. Additionally, both theories have global symmetries relating certain operators of these sets, i.e. some operators within a set have the same scaling dimension. Global $U(1)$ symmetry relates the real and imaginary parts of monopole operators in both theories. Flavor symmetry on the fermionic side relates the two types of monopole operators while a $SU(2)$ symmetry on the bosonic side implies that all three components of the bilinear $z^\dagger \sigma z$ share the same scaling dimension. Taking into account these global symmetries and the conjectured duality, it is deduced that all operators above should have the same scaling dimension. Said otherwise, the duality predicts an emergent $SO(5)$ symmetry at the fixed point of these theories. The duality can thus be tested by comparing the monopole scaling dimension obtained above to other scaling dimensions conjectured to be the same.

The scaling dimension of the monopole operator with $q = 1/2$ in $\text{QED}_3 - \text{GN}$ for $2N_f = 2$ fermion flavors is $\Delta_{\mathcal{M}_{q=1/2}^{\text{CP}^1}}^{\text{QED}_3 - \text{GN}} = 2N_f(0.26510) \sim 0.53$. We compare this value to results in the literature for the other scaling dimensions. For the monopole operator with minimal magnetic charge in the bosonic theory CP^{N_b-1} with $N_b = 2$, it was found in a similar computation using the state-operator correspondence that $\Delta_{\mathcal{M}_{q=1/2}^{\text{CP}^{N_b-1}}} = 0.1245922N_b + 0.05992 \sim 0.31$ [40]. Note that this result violates the unitary bound; in addition, it is small when compared to other results in the literature. Using a large N_b expansion in a functional renormalization group analysis [52], it was found that $\Delta_{\text{Néel}} \equiv \Delta_{z^\dagger \sigma z} = 0.61$, which is closer to our 0.53. On the numerical front, the scaling dimensions of the VBS order parameter $\Delta_{\text{VBS}} \equiv \Delta_{\mathcal{M}_{q=1/2}^{\text{CP}^1}}$ and the Néel

order parameter $\Delta_{\text{Néel}}$ were found to be in the range $\Delta_{\text{VBS}, \text{Néel}} \in [0.60, 0.68]$ [53–57]. On the fermionic side, a large N_f expansion suggest that the scaling dimension of the boson might be in the range $\Delta_\phi \in [0.59, 0.65]$ [58]. While these last results do not seem far off from the scaling dimension of the monopole operator that we obtain, a more precise computation could help clarify the situation.

VI. RENORMALIZATION GROUP ANALYSIS OF THE CRITICAL FIXED POINT

We study more thoroughly the critical fixed point by considering the Yukawa theory that is the UV completion of the $\text{QED}_3 - \text{cHGN}$ model (5). This model is called $\text{QED}_3 - \text{cHGNY}$ and is defined by the following bare Euclidean lagrangian

$$\mathcal{L} = -\bar{\Psi} \not{\partial} \Psi + \frac{1}{2} (\epsilon_{\mu\nu\rho} \partial_\nu a_\rho)^2 + \frac{1}{2} (\partial_\mu \phi)^2 \\ + ie \bar{\Psi} \not{\phi} \Psi + h \phi \cdot \bar{\Psi} \sigma \Psi + \frac{1}{2} m_\phi^2 \phi^2 + \lambda (\phi^2)^2. \quad (72)$$

In this section, we consider the non-compact version of QED_3 . As before, Ψ denotes the spinor with $2N_f$ flavors of two-component Dirac fermion field and ϕ is a boson field with $N_b = 3$ components. We perform the renormalization group (RG) analysis for general N_f and N_b , and then we specialize to $N_b = 3$ and $2N_f = 4$, which are relevant parameters for certain quantum magnets. For simplicity, we keep referring to this model as $\text{QED}_3 - \text{cHGNY}$ although we don't fix $N_b = 3$ from the outset. RG studies for similar quantum field theories have been considered before. For example, a gauged theory with a valley-dependent cHGNY-like interaction, $\phi \bar{\Psi} \mu_z \sigma \Psi$, and with $2N_f = 4$ fermion flavors was studied to leading order in $\epsilon = 4 - d$ expansion [18]. Here, d is the spacetime dimension.

The analysis was also done in the ungauged theory, i.e. the cHGNY model, with general N_f at four loops in the $\epsilon = 4 - d$ expansion [59] and to order $1/N_f^2$ [60]. The $\text{QED}_3 - \text{GN}$ was also considered for general N_f using dimensional regularization at one-loop [61], three-loop [62] and four-loop [63] and to order $1/N_f^2$ [58; 64; 65]. In the last reference, a spin-dependent Yukawa interaction term with $N_b = 1$, $\phi \bar{\Psi} \sigma_z \Psi$, has also been considered. See [66] for a comprehensive review on large- N_f methods.

A. Setup

The first step in our RG study is to write the renormalized Euclidean lagrangian

$$\begin{aligned}\mathcal{L} = & -Z_\psi \bar{\Psi} \not{\partial} \Psi + \frac{1}{2} Z_a (\epsilon_{\mu\nu\rho} \partial_\nu a_\rho)^2 + \frac{1}{2} Z_\phi (\partial_\mu \phi)^2 \\ & + Z_e (ie) \mu^{\frac{4-d}{2}} \bar{\Psi} \not{\partial} \Psi + Z_h h \mu^{\frac{4-d}{2}} \phi \cdot \bar{\Psi} \sigma \Psi \\ & + \frac{1}{2} Z_{m_\phi}^2 m_\phi^2 \mu^2 \phi^2 + Z_\lambda \lambda \mu^{4-d} (\phi^2)^2,\end{aligned}\quad (73)$$

where we introduced wave function renormalization constants Z_ψ , Z_ϕ and Z_a as well as vertex renormalization constants Z_e , Z_h , $Z_{m_\phi}^2$ and Z_λ . Coupling constants are also rescaled by powers of energy μ factoring out their naive scaling dimension. The renormalized fields are obtained by a rescaling of the bare fields

$$\Psi_0 = \sqrt{Z_\psi} \Psi, \quad \phi_0 = \sqrt{Z_\phi} \phi, \quad (a_\mu)_0 = \sqrt{Z_a} a_\mu. \quad (74)$$

From (74), analog relations between the renormalized coupling constants $(e^2, h^2, \lambda) \equiv (c_1, c_2, c_3) = \mathbf{c}$ the bare coupling constants are obtained

$$e^2 = e_0^2 \mu^{d-4} Z_a, \quad (75)$$

$$h^2 = h_0^2 \mu^{d-4} Z_\psi^2 Z_\phi Z_h^{-2}, \quad (76)$$

$$\lambda = \lambda_0 \mu^{d-4} Z_\phi^2 Z_\lambda^{-1}, \quad (77)$$

where the Ward identity, $Z_\psi^2 Z_e^{-2} = 1$, was used to simplify the renormalization of the gauge charge e^2 . We also add a gauge fixing term $\mathcal{L}_{\text{g.f.}} = (\partial_\mu a_\mu)^2 / (2\xi)$ to ensure physical quantities are gauge independent. We have explicitly written a quadratic boson term since, as we discussed in Sec.IIB, the mass is the tuning parameter for the phase transition. We first study the RG flow equations at the critical value of the boson mass, $m_\phi^c = 0$. Later on, we incorporate the boson mass term, along with fermion bilinears, as perturbations away from the QCP.

By rescaling the energy $\mu \rightarrow \mu e^{-l}$ in (75 - 77), we can analyze how the coupling constants vary with the scale factor [67]. The RG flow equation are found by differentiating the renormalized coupling constants with respect to the scale factor, i.e. by obtaining the beta functions $\beta_{c_I} = dc_I/dl$ with $I \in \{1, 2, 3\}$

$$\beta_{e^2} \equiv \frac{de^2}{dl} = (4 - d - \gamma_a) e^2, \quad (78)$$

$$\beta_{h^2} \equiv \frac{dh^2}{dl} = (4 - d - 2\gamma_\psi - \gamma_\phi + 2\gamma_h) h^2, \quad (79)$$

$$\beta_{\lambda^2} \equiv \frac{d\lambda}{dl} = (4 - d - 2\gamma_\phi + \gamma_\lambda) \lambda, \quad (80)$$

where the coefficients γ_{x_i} with $x_i \in \{\psi, \phi, a, h, \lambda\}$ are defined as

$$\gamma_{x_i} = -\frac{d \ln Z_{x_i}}{dl}. \quad (81)$$

These coefficients γ_{x_i} are obtained in App. C and allow to find the following RG flow equations

$$\frac{de^2}{dl} = (4 - d) e^2 - \frac{4N_f}{3} e^4, \quad (82)$$

$$\begin{aligned}\frac{dh^2}{dl} = & (4 - d) h^2 + 8 \left(1 - \frac{1}{d}\right) e^2 h^2 \\ & - 2 \left(N_f + 2 - \frac{2N_b}{d}\right) h^4,\end{aligned}\quad (83)$$

$$\frac{d\lambda}{dl} = (4 - d) \lambda - 4N_f h^2 \lambda + N_f h^4 - 4(N_b + 8) \lambda^2, \quad (84)$$

where the coupling constants have been rescaled to eliminate a loop integral factor. We will first find the fixed points of the RG flow, that is the critical coupling constants $(e_*^2, h_*^2, \lambda_*) \equiv \mathbf{c}_*$ for which the beta functions vanish, $\beta_{c_I} = 0$. The QED₃ - cHGNY infrared fixed point corresponding to the QCP will be found, and we will evaluate critical exponents at this point.

B. Fixed points in the $1/N_f$ expansion

We first control the convergence of the flow by a $1/N_f$ expansion. Setting $d = 3$ and assuming that coupling constants are order $1/N_f$, the flow equations become

$$\frac{de^2}{dl} = e^2 - \frac{4N_f}{3} e^4, \quad (85)$$

$$\frac{dh^2}{dl} = h^2 - 2N_f h^4, \quad (86)$$

$$\frac{d\lambda}{dl} = \lambda - 4N_f h^2 \lambda + N_f h^4. \quad (87)$$

This set of equations leads to the subset of fixed points shown in Tab. II. This excludes Wilson-Fisher type fixed points for which λ is not controlled by the $1/N_f$ expansion. The linearized RG flow equations around a fixed point \mathbf{c}^* yields a matrix equation for the coupling constant perturbations

$$\frac{d}{dl} (c_I - c_I^*) = \sum_{J=1,2,3} M_{IJ} (c_J - c_J^*), \quad (88)$$

where M_{IJ} is the stability matrix

$$M_{IJ} = \left. \frac{\partial \beta_{c_I}}{\partial c_J} \right|_{\mathbf{c}=\mathbf{c}^*}. \quad (89)$$

Eigenvectors of this matrix equation yield proper directions in the parameter space of couplings $\{e^2, h^2, \lambda\}$. The related eigenvalues λ_I indicate relevant ($\lambda_I > 0$), marginal ($\lambda_I = 0$), or irrelevant ($\lambda_I < 0$) perturbations. An infrared fixed point is characterized by irrelevant perturbations in all proper directions. For the theory we study, there is a unique infrared fixed point which, at

Table II: Fixed points obtained at leading order in the $1/N_f$ expansion of RG flow equations (85 - 87). There are four such fixed points, where G stands for “Gaussian”. This excludes Wilson-Fisher type fixed points which are not controlled by the $1/N_f$ expansion.

Fixed points	e_*^2	h_*^2	λ_*
G	0	0	0
QED ₃	$\frac{3}{4N_f}$	0	0
cHGNy	0	$\frac{1}{2N_f}$	$\frac{1}{4N_f}$
QED ₃ - cHGNy	$\frac{3}{4N_f}$	$\frac{1}{2N_f}$	$\frac{1}{4N_f}$

order $1/N_f$, is given by

$$e_*^2 = \frac{3}{4N_f}, \quad h_*^2 = \frac{1}{2N_f}, \quad \lambda_* = \frac{1}{4N_f}. \quad (90)$$

At this infrared fixed point, called QED₃ - cHGNy, all critical coupling constants are non-zero.

C. RG study in the $\epsilon = 4 - d$ expansion

We now use a dimensional regularization to control the RG flow. We study the theory at finite N_f by working near the upper critical number of spacetime dimensions $d = 4 - \epsilon$, where ϵ is treated as a small expansion parameter. Assuming the coupling constants are $\mathcal{O}(\epsilon)$, we obtain the flow equations in the ϵ expansion

$$\frac{de^2}{dl} = \epsilon e^2 - \frac{4N_f}{3} e^4, \quad (91)$$

$$\frac{dh^2}{dl} = \epsilon h^2 + 6e^2 h^2 - (2N_f + 4 - N_b) h^4, \quad (92)$$

$$\frac{d\lambda}{dl} = \epsilon \lambda + N_f h^4 - 4N_f h^2 \lambda - 4(N_b + 8) \lambda^2. \quad (93)$$

The corresponding physical fixed points are shown in Tab. III, where we have defined

$$\begin{aligned} f_{N_f, N_b} &= [4N_f^4 + 4(5N_b + 46)N_f^3 + 324(N_b + 8)N_f \\ &\quad + (N_b^2 + 172N_b + 1348)N_f^2]^{1/2}, \quad (94) \\ f'_{N_f, N_b} &= [4N_f^2 + 4(5N_b + 28)N_f + (N_b - 4)^2]^{1/2}. \quad (95) \end{aligned}$$

By studying the linearized RG flow around the fixed points, one can again show that the QED₃ - cHGNy is an infrared fixed point. We note in this case that the infrared fixed point is in the physical region $h^2 > 0$ only if $2N_f - N_b + 4 > 0$.

The flow in the $(\lambda/\epsilon, h^2/\epsilon)$ plane with e^2 fixed to its two possible critical values is shown Fig. 7. In particular, the flow from the QED₃ fixed point ($h^2 = \lambda = 0$) to the QED₃ - cHGNy fixed point is shown in Fig. 7(a). Setting $N_b = 3$, this infrared fixed point is given by following

critical coupling constants

$$e_*^2 = \frac{3}{4N_f} \epsilon, \quad (96)$$

$$h_*^2 = \frac{2N_f + 9}{2N_f(2N_f + 1)} \epsilon, \quad (97)$$

$$\lambda_* = \frac{-2N_f^2 - 17N_f + f_{N_f, 3}}{88N_f(2N_f + 1)} \epsilon, \quad (98)$$

where

$$f_{N_f, 3} = [N_f(4N_f^3 + 244N_f^2 + 1873N_f + 3564)]^{1/2}. \quad (99)$$

Expanding in powers of $1/N_f$ and setting $\epsilon = 1$, the infrared fixed point corresponds to the previous $1/N_f$ result (90).

1. Critical exponents at the quantum critical point

We now compute the critical exponents at the infrared fixed point. The scaling dimension of an operator $\mathcal{O}(x)$ at the QCP is defined by the following expectation value

$$\langle \mathcal{O}(x_1) \mathcal{O}^\dagger(x_2) \rangle \propto \frac{1}{|x_1 - x_2|^{2\Delta_{\mathcal{O}}}}, \quad (100)$$

Using scaling arguments, one can write a naive dimension $\Delta_{\mathcal{O}}^0$. This value is corrected by an anomalous dimension $\eta_{\mathcal{O}}$ once interactions are taken into account

$$\Delta_{\mathcal{O}} = \Delta_{\mathcal{O}}^0 + \frac{\eta_{\mathcal{O}}}{2}. \quad (101)$$

We start by studying the anomalous dimensions of the fields η_{Φ} with $\Phi \in \{\phi, \psi, a\}$. These quantities are found by evaluating the corresponding coefficients γ_{Φ} (81) at the QCP, that is $\eta_{\Phi} = \gamma_{\Phi}|_{\mathbf{c}=\mathbf{c}_{\text{QCP}}}$. First, we write the general expressions for these coefficients obtained in App. C

$$\gamma_{\phi} = 2N_f h^2, \quad (102)$$

$$\gamma_{\psi} = \left(d + \xi - 5 + \frac{4}{d}\right) e^2 + \left(1 - \frac{2}{d}\right) N_b h^2, \quad (103)$$

$$\gamma_a = \frac{4N_f}{3} e^2. \quad (104)$$

Table III: Fixed points obtained at leading order in the $\epsilon = 4 - d$ expansion of RG flow equations (91 - 93). f_{N_f, N_b} and f'_{N_f, N_b} are defined in Eqs. (94, 95), respectively. There are six fixed points, where G stands for “Gaussian” and WF for “Wilson-Fisher”.

Fixed points	e_*^2	h_*^2	λ_*
G	0	0	0
QED ₃	$\frac{3}{4N_f}\epsilon$	0	0
WF	0	0	$\frac{1}{4(N_b + 8)}\epsilon$
QED ₃ - WF	$\frac{3}{4N_f}\epsilon$	0	$\frac{1}{4(N_b + 8)}\epsilon$
cHGNY	0	$\frac{1}{2N_f - N_b + 4}\epsilon$	$\frac{f'_{N_f, N_b} - 2N_f - N_b + 4}{8(N_b + 8)(2N_f - N_b + 4)}\epsilon$
QED ₃ - cHGNY	$\frac{3}{4N_f}\epsilon$	$\frac{2N_f + 9}{2N_f(2N_f - N_b + 4)}\epsilon$	$\frac{f_{N_f, N_b} - 2N_f^2 - (N_b + 14)N_f}{8N_f(N_b + 8)(2N_f - N_b + 4)}\epsilon$

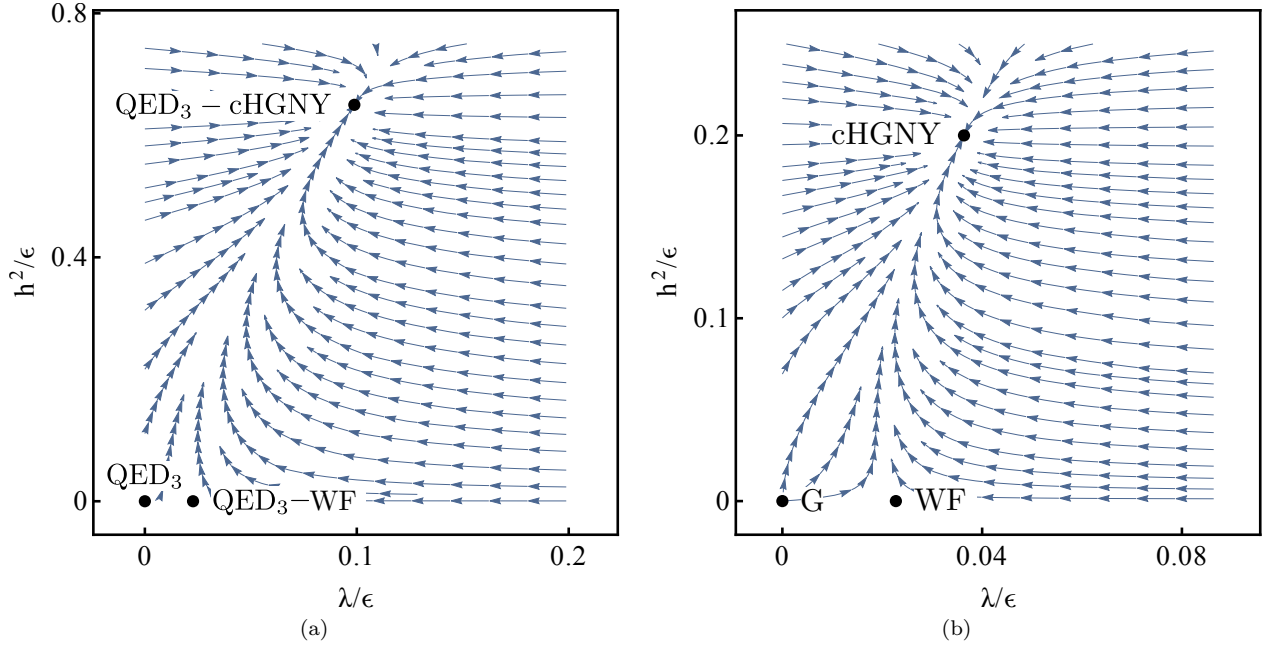


Figure 7: RG flow for $2N_f = 4$ and $N_b = 3$ in the $(\lambda/\epsilon, h^2/\epsilon)$ plane to leading order in $\epsilon = 4 - d$. a) Flow for $e^2 = 3\epsilon/4N_f$; b) Flow for $e^2 = 0$.

Replacing the coupling constants in Eqs. (102 - 104) by their critical value at the QED₃ - cHGNY fixed point in Tab. III, we obtain the anomalous dimensions

$$\eta_\phi = \frac{2N_f + 9}{2N_f - N_b + 4}\epsilon, \quad (105)$$

$$\eta_\psi = \frac{N_b(2N_f - 3\xi + 9) + 6\xi(N_f + 2)}{4N_f(2N_f - N_b + 4)}\epsilon, \quad (106)$$

$$\eta_a = \epsilon. \quad (107)$$

Note that the anomalous dimension of the fermion depends on the gauge fixing parameter ξ , but this is expected since it is not a gauge invariant quantity. The gauge field anomalous dimension is ϵ which implies that the one-loop corrected gauge field propagator is

$\langle a_\mu(p)a_\nu(-p) \rangle \sim |p|^{-1}$ once we set $\epsilon = 1$. By setting $e_*^2 \neq 0$ in the gauge charge flow equation (78), it is seen that the one-loop result we found, $\eta_a = \epsilon$, is actually valid to all orders. This is again a consequence of the Ward identity. Now, setting $N_b = 3$ in the anomalous dimensions (105 - 106), we obtain

$$\eta_\phi = \frac{2N_f + 9}{2N_f + 1}\epsilon, \quad \eta_\psi = \frac{3(2(\xi + 1)N_f + \xi + 9)}{4N_f(2N_f + 1)}\epsilon. \quad (108)$$

Setting $2N_f = 4$, we obtain

$$\eta_\phi = \frac{13}{5}\epsilon, \quad \eta_\psi = \frac{3(5\xi + 13)}{40}\epsilon. \quad (109)$$

Setting $\epsilon = 1$, we find $\Delta_\phi = (d - 2)/2 + \eta_\phi/2 \approx 1.8$.

We now study the scaling dimension of mass operators by introducing mass perturbations at the QCP

$$\Delta\mathcal{L} = \frac{1}{2}Z_{m_\phi^2}m_\phi^2\phi^2 + Z_{m_\psi}m_\psi\bar{\Psi}\Psi + Z_{\tilde{m}_\psi}\tilde{m}_\psi(\hat{n} \cdot \bar{\Psi}\sigma\Psi), \quad (110)$$

where \hat{n} is a unit vector indicating the direction of the spin-Hall bilinear perturbation. We do not include a valley-Hall bilinear $\bar{\Psi}\mu_A\Psi$, where $A \in \{1, 2, \dots, N_f\}$, since its scaling dimension is the same as the $SU(2N_f)$ symmetric bilinear $\bar{\Psi}\Psi$ at leading order in $\epsilon = 4 - d$. The masses we introduced can be related to bare masses like we did with the other coupling constants

$$m_\phi^2 = (m_\phi^2)_0 \mu^2 Z_\phi Z_{m_\phi^2}^{-1}, \quad (111)$$

$$m_\psi = (m_\psi)_0 \mu Z_\psi Z_{m_\psi}^{-1}, \quad (112)$$

$$\tilde{m}_\psi = (\tilde{m}_\psi)_0 \mu Z_\psi Z_{\tilde{m}_\psi}^{-1}. \quad (113)$$

The RG flow equations follow from these relations are

$$\frac{dm_\phi^2}{dl} = (2 - \gamma_\phi + \gamma_{m_\phi^2}) m_\phi^2, \quad (114)$$

$$\frac{dm_\psi}{dl} = (1 - \gamma_\psi + \gamma_{m_\psi}) m_\psi, \quad (115)$$

$$\frac{d\tilde{m}_\psi}{dl} = (1 - \gamma_\psi + \gamma_{\tilde{m}_\psi}) \tilde{m}_\psi, \quad (116)$$

where the γ_{x_i} with $x_i \in \{\phi, \psi, m_\phi^2, m_\psi, \tilde{m}_\psi\}$ are defined in Eq. (81). Using results of App. C, the RG flow equations become

$$\frac{dm_\phi^2}{dl} = (2 - 2N_f h^2 - 4(N_b + 2)\lambda) m_\phi^2, \quad (117)$$

$$\frac{dm_\psi}{dl} = \left(1 + 4\left(\frac{d-1}{d}\right)e^2 + 2N_b\left(\frac{1-d}{d}\right)h^2\right) m_\psi, \quad (118)$$

$$\frac{d\tilde{m}_\psi}{dl} = \left(1 + 4\left(\frac{d-1}{d}\right)e^2 + 2\left(\frac{N_b-d}{d}\right)h^2\right) \tilde{m}_\psi. \quad (119)$$

When the coupling constants are evaluated at their QED_3 - cHGN critical value, the RG flow of the masses is controlled by the scaling dimension of the related mass operators at the QCP

$$\frac{dm_\phi^2}{dl} = (d - \Delta_{\phi^2}) m_\phi^2, \quad (120)$$

$$\frac{dm_\psi}{dl} = (d - \Delta_{\bar{\Psi}\Psi}) m_\psi, \quad (121)$$

$$\frac{d\tilde{m}_\psi}{dl} = (d - \Delta_{\bar{\Psi}\sigma_a\Psi}) \tilde{m}_\psi. \quad (122)$$

We first study the ϕ^2 perturbation. The phase transition is controlled by the mass m_ϕ^2 auxiliary boson and the correlation length exponent $\nu^{-1} = d - \Delta_{\phi^2}$ is obtained

by evaluating (117) at the QCP

$$\nu^{-1} = 2 - \frac{2N_f + 9}{2N_f - N_b + 4}\epsilon - \frac{(N_b + 2)(f_{N_f, N_b} - N_f(2N_f + N_b + 14))}{2N_f(N_b + 8)(2N_f - N_b + 4)}\epsilon. \quad (123)$$

Setting $N_b = 3$, we obtain

$$\nu^{-1} = 2 - \frac{34N_f^2 + 113N_f + 5f_{N_f, 3}}{22N_f(2N_f + 1)}\epsilon, \quad (124)$$

which gives the correct $N_f \rightarrow \infty$ limit: $\nu = 1$. Setting $2N_f = 4$, we obtain

$$\nu^{-1} = 2 - 4.577\epsilon. \quad (125)$$

Setting $\epsilon = 1$, our one loop result yields a negative correlation length exponent. This is was also observed for the QED_3 - GNY model in Ref. [61] where a dimensional regularization around $d = 2 + \epsilon$ was also performed to do an interpolation and obtain a positive correlation length exponent. One could also go further in the loop expansion to obtain a physical result in the $\epsilon \rightarrow 1$ limit. However, a physical estimate for ν can be obtained by inverting ν^{-1}

$$\nu = \frac{1}{2} + \frac{34N_f^2 + 113N_f + 5f_{N_f, 3}}{88N_f(2N_f + 1)}\epsilon \Big|_{2N_f=4} = \frac{1}{2} + 1.144\epsilon. \quad (126)$$

Setting $\epsilon = 1$ now yields the physical result $\nu = 1.644$. Inverting this exponent once again, we obtain the scaling dimension of ϕ^2 which is given by $\Delta_{\phi^2} = d - \nu^{-1} \approx 2.392$.

We now turn our attention to the fermion bilinears perturbations. Evaluating (118, 119) with critical couplings of the QED_3 - cHGN fixed point shown at leading order in ϵ in Tab. III, we find the scaling dimensions at the QCP are given by

$$\Delta_{\bar{\Psi}\Psi} = 3 - \frac{4N_f^2 - (5N_b - 17)N_f - 18(N_b - 1)}{2N_f(2N_f - N_b + 4)}\epsilon, \quad (127)$$

$$\Delta_{\bar{\Psi}\sigma_a\Psi} = 3 - \frac{4N_f - N_b + 13}{2(2N_f - N_b + 4)}\epsilon. \quad (128)$$

Setting $N_b = 3$, we obtain

$$\Delta_{\bar{\Psi}\Psi} = 3 - \frac{2N_f^2 + N_f - 18}{N_f(2N_f + 1)}\epsilon, \quad (129)$$

$$\Delta_{\bar{\Psi}\sigma_a\Psi} = 3 - \frac{2N_f + 5}{2N_f + 1}\epsilon. \quad (130)$$

Setting $2N_f = 4$, this becomes

$$\Delta_{\bar{\Psi}\Psi} = 3 + \frac{4}{5}\epsilon, \quad \Delta_{\bar{\Psi}\sigma_a\Psi} = 3 - \frac{9}{5}\epsilon. \quad (131)$$

Once we set $\epsilon = 1$, the spin-Hall bilinear is relevant at the QCP, $\Delta_{\bar{\Psi}\sigma_a\Psi} = 1.2$, but the symmetric bilinear is not, $\Delta_{\bar{\Psi}\Psi} = 3.8$. This contradicts what we obtain by taking the large N_f limit in (129) since the scaling dimension $\Delta_{\bar{\Psi}\Psi}|_{N_f \rightarrow \infty} = 3 - \epsilon$ then implies a relevant operator for $\epsilon = 1$. It is expected that higher order corrections in $\epsilon = 4 - d$ would render $\bar{\Psi}\Psi$ relevant.

The critical exponents we found are compiled in Tab. IV. In principle, many of our scaling dimensions should agree with the results in Ref. [18] for $2N_f = 4$ and $N_b = 3$ since the theory considered in this case is almost the same. We find small discrepancies attributable the RG flow equation for the Yukawa coupling, i.e. using their normalization, our Eq. (92) doesn't match Eq. (27) in Ref. [18]. Fortunately, the mismatch comes from diagrams which are independent of the number of boson components, thus we can compare with studies of the QED₃ – GNY model (see for example Ref. [61]) which confirm our result. We did other verifications for different regions of the parameter space of our theory. First, we considered the ungauged theory $e^2 = 0$ where the QCP point is given by the cHGN fixed point. Setting $N_b = 3$, the fixed points, the RG flow equations and the critical exponents match those of the cHGN model presented in Ref. [59]. The fermion bilinear scaling dimensions, which were not computed in this last reference, match the leading order results in $1/N_f$ of [60]. We also verified the gauged theory when $N_b = 1$. In this model, the spin-Hall bilinear scaling dimension $\Delta_{\bar{\Psi}\sigma_a\Psi}$ is equal, at one-loop order, to the symmetric bilinear scaling dimension $\Delta_{\bar{\Psi}\Psi}$ in QED₃ – GNY. We find agreement with the results obtained in $\epsilon = 4 - d$ expansions presented in Refs. [59; 61], and by taking the large N_f limit in our ϵ expansion and comparing to results obtained with large N_f expansions in Refs. [64; 65; 68]. As noted in Ref. [63], the result for $\Delta_{\bar{\Psi}\Psi}$ disagrees with the one presented in [69]. We find that the latter result would be obtained if the renormalization of the fermion mass included a Hartree diagram. This contribution is not generated in Wilsonian RG.

Table IV: Critical exponents at the QED₃ – cHGN fixed point with $N_b = 3$ at leading order in $\epsilon = 4 - d$. $f_{N_f,3}$ is defined in (99). The scaling dimension of valley-Hall bilinears is $\Delta_{\bar{\Psi}\mu_A\Psi} = \Delta_{\bar{\Psi}\Psi}$ where $A \in \{1, 2, \dots, N_f\}$.

		$2N_f = 4$	$2N_f = 4$ $\epsilon = 1$
η_ϕ	$\frac{2N_f + 9}{2N_f + 1}\epsilon$	2.6ϵ	2.6
ν	$\frac{1}{2} + \frac{34N_f^2 + 113N_f + 5f_{N_f,3}}{88N_f(2N_f + 1)}\epsilon$	$\frac{1}{2} + 1.144\epsilon$	1.644
$\Delta_{\bar{\Psi}\Psi}$	$3 - \frac{2N_f^2 + N_f - 18}{N_f(2N_f + 1)}\epsilon$	$3 + 0.8\epsilon$	3.8
$\Delta_{\bar{\Psi}\sigma_a\Psi}$	$3 - \frac{2N_f + 5}{2N_f + 1}\epsilon$	$3 - 1.8\epsilon$	1.2

VII. QUANTUM PHASE TRANSITION IN THE KAGOME MAGNET

The QED₃ – cHGN model considered in the previous sections finds a natural application in quantum magnets where the underlying lattice implies the compactness of the emergent gauge field and the existence of the monopole operators. We specialize our analysis to the quantum magnet on the Kagome lattice. We first review how a DSL emerges as a possible ground state of the Kagome Heisenberg Antiferromagnet (KHAFM) model. This simple Hamiltonian serves as a starting point to describe the magnetic Cu atoms in Hebertsmithite $\text{ZnCu}_3(\text{OH})_6\text{Cl}_2$ [70]. We also review the confinement-deconfinement transition from this DSL to a $\mathbf{q} = 0$ coplanar antiferromagnetic phase. We then examine the properties of the monopole operators perturbations which drive this quantum phase transition.

A. Emergent QED₃

The Hamiltonian of the KHAFM is

$$H_H = J_1 \sum_{\langle ij \rangle} \mathbf{S}_i \cdot \mathbf{S}_j, \quad (132)$$

where $J_1 > 0$ gives the coupling strength of AFM interactions between nearest neighbors of the Kagome lattice. The emergent fractional spin excitations and gauge field in this model arise due to fractionalization. This phenomenon is studied using a parton construction. The spin operator on site i is decomposed as

$$\mathbf{S}_i = \frac{1}{2} f_{i,s}^\dagger \boldsymbol{\sigma}_{ss'} f_{i,s'}, \quad (133)$$

where $f_{i,s}$ is a slave-fermion (spinon) with spin $s \in \{\uparrow, \downarrow\}$ and $\boldsymbol{\sigma}$ is a vector of Pauli matrices acting on this spin space. The spinon variables introduce a U(1) gauge redundancy¹² through the symmetry transformation $f_{i,s} \rightarrow e^{i\theta_i} f_{i,s}$. The new Hilbert space is doubled compared to the original spin model, therefore an occupation constraint, $f_{i,s}^\dagger f_{i,s} = 1$, must be imposed. A QSL arises when spinon and gauge degrees of freedom are deconfined. The ground state of the KHAFM is not yet well established. Many numerical studies indicate a U(1) spin liquid for the ground state [12; 14–16; 71; 72] while other investigations point towards a \mathbb{Z}_2 spin liquid [73–78]. In the latter class of spin liquids, the U(1) gauge symmetry is broken due to a non-vanishing expectation value of spinon pairs $\langle f_i^\dagger f_j^\dagger \rangle$.

We focus our attention on U(1) spin liquids. Using the spinon decomposition (133) and applying the occupation constraint, the Hamiltonian developed around the

¹² There is a larger SU(2) gauge symmetry, but the U(1) subgroup is sufficient for our discussion.

hopping expectation value $\langle f_{is}^\dagger f_{js} \rangle \neq 0$ becomes

$$\tilde{H}_H = - \sum_{\langle ij \rangle} t_{ij} e^{i a_{ij}} f_i^\dagger f_j + \text{h.c.}, \quad (134)$$

where the sum on spin indices is now implicit, $t_{ij} = J_1 \langle f_i^\dagger f_j \rangle / 2$ and a_{ij} are the phase fluctuations around the expectation value $\langle f_i^\dagger f_j \rangle$. The U(1) gauge symmetry is preserved if the phase fluctuation transforms as $a_{ij} \rightarrow a_{ij} + \theta_i - \theta_j$. This degree of freedom is thus a dynamical U(1) gauge field.

Among the possible realizations of a U(1) spin liquid, the candidate ground state is obtained with the π -flux pattern of the bond orders which is depicted in Fig. 8. This pattern defines the ground-state called U(1)

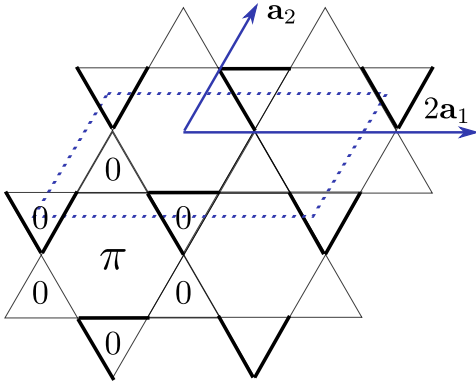


Figure 8: π -flux pattern on the Kagome lattice. Bold bonds and regular bonds have opposite signs for their corresponding hopping parameters.

Dirac spin liquid (DSL) and which has 4 Dirac cones at the Fermi level [79]. The low energy limit is described by QED₃ with $2N_f = 4$ flavors of massless two-component Dirac fermions, two spin components and two nodes $\pm \mathbf{Q}$ in momentum space [79]. An eight-component spinor regrouping all degrees of freedom can be written as $\Psi = (\psi_{\uparrow, \mathbf{Q}}, \psi_{\uparrow, -\mathbf{Q}}, \psi_{\downarrow, \mathbf{Q}}, \psi_{\downarrow, -\mathbf{Q}})^T$. Vectors of Pauli matrices acting on $SU(2)_{\text{spin}}$ and $SU(2)_{\text{valley}}$ subspaces, respectively labeled as $\boldsymbol{\sigma}$ and $\boldsymbol{\mu}$, allow to form spin and valley vectors, $\bar{\Psi} \boldsymbol{\sigma} \Psi$ and $\bar{\Psi} \boldsymbol{\mu} \Psi$. Specifically, the third Pauli matrices in each subspace act as $\sigma_z = |\uparrow\rangle \langle \uparrow| - |\downarrow\rangle \langle \downarrow|$ and $\mu_z = |+\mathbf{Q}\rangle \langle +\mathbf{Q}| - |-\mathbf{Q}\rangle \langle -\mathbf{Q}|$. In similar fashion, Dirac matrices acting on the two-dimension spinor space are represented by Pauli matrices, $\gamma_\mu = (\tau_3, \tau_2, -\tau_1)$. The transformations of these fermions under Kagome lattice symmetries and time reversal are shown in Tab. V [19].

B. Antiferromagnetic order parameter

We now modify the lattice model to include a next-nearest neighbor AFM coupling J_2 . The resulting Hamil-

tonian describes the spin-1/2 $J_1 - J_2$ Heisenberg model

$$H' = J_1 \sum_{\langle ij \rangle} \mathbf{S}_i \cdot \mathbf{S}_j + J_2 \sum_{\langle\langle ij \rangle\rangle} \mathbf{S}_i \cdot \mathbf{S}_j. \quad (135)$$

When the ratio J_2/J_1 is sufficiently large, the Kagome frustrated magnet orders to a $\mathbf{q} = 0$ AFM coplanar phase [15; 80; 81] shown in Fig. 9. The order parameter can

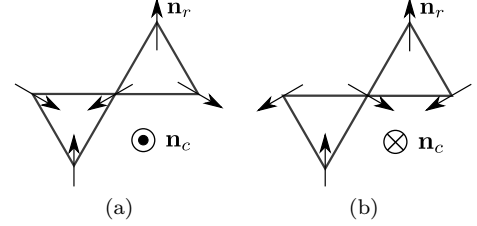


Figure 9: Antiferromagnetic $\mathbf{q} = 0$ non-collinear phase with a complex order parameter $\mathbf{n} = \mathbf{n}_r + i(\mathbf{n}_r \times \mathbf{n}_c)$ with a) positive chirality; b) negative chirality.

be described as a complex vector $\mathbf{n} = \mathbf{n}_r + i(\mathbf{n}_r \times \mathbf{n}_c)$ whose real part encodes the orientation of the spin on one of Kagome's three sub-lattices. On each triangle, the two remaining spins are separated by 120° angles with chirality determined by \mathbf{n}_c . The transformation properties of this vector are shown in Tab. VI.

We now show that monopole operators with spin quantum numbers have the same transformation properties as the AFM order parameter shown in Tab. VI. This was first argued in Ref. [19]. A comprehensive study of the quantum numbers of monopole operators on the square, triangular honeycomb and Kagome lattices can be found in Ref. [31; 82]. One important contribution of this work was to verify numerically the contribution of the $U(1)_{\text{top}}$ charge for the space rotation. This amounts to deducing how the topologically charged Dirac sea transforms under the system symmetries. This result can be combined with the transformation properties of the zero modes creation operators to obtain the transformation properties of flux operators. This approach is well explained in Ref. [83]. We apply this procedure to the case of the Kagome lattice.

Here, we restrict the discussion to monopoles with minimal magnetic charge $q = 1/2$. This means there are four zero modes, two of which must be filled. The $q = 1/2$ flux operators take the form

$$\Phi_+^\dagger \sim f_{+,s,v}^\dagger f_{+,s',v'}^\dagger \widetilde{\mathcal{M}}_+^\dagger, \quad (136)$$

where the label $+$ gives the sign of the magnetic charge, $f_{+,s,v}^\dagger$ is a zero mode creation operator and $\widetilde{\mathcal{M}}_+^\dagger$ defines a bare 2π -flux creating operator, an operator similar to a monopole operator but with all the zero modes empty (in what follows, we refer to it as the bare monopole operator). The six different zero modes filling can be organized as a triplet of $SU(2)_{\text{valley}}$ and a triplet of $SU(2)_{\text{spin}}$, yield-

Table V: Transformation properties of spinons under discrete symmetries of the KHAfM [19] where $\mu_{C_6} = (\mu_1 + \mu_2 - \mu_3)/\sqrt{3}$ and $\mu_{\mathcal{R}_y} = -(\mu_1 + \mu_3)/\sqrt{2}$.

	$T_{\mathbf{a}_1}$	$T_{\mathbf{a}_2}$	\mathcal{R}_y	C_6	\mathcal{T}
$\Psi \rightarrow$	$i\mu_2\Psi$	$i\mu_3\Psi$	$\exp\left(\frac{i\pi}{2}\mu_{\mathcal{R}_y}\right)(i\tau_1)\Psi$	$\exp\left(\frac{2\pi i}{3}\mu_{C_6}\right)\exp\left(\frac{i\pi}{6}\tau_3\right)\Psi$	$(i\sigma_2)(-i\mu_2)(i\tau_2)\Psi$

Table VI: Transformation properties of the $\mathbf{q} = 0$ coplanar AFM order \mathbf{n} shown in Fig. 9 under Kagome lattice discrete symmetries and time reversal[19].

	$T_{\mathbf{a}_1}$	$T_{\mathbf{a}_2}$	R_y	C_6	\mathcal{T}
$\mathbf{n} \rightarrow$	\mathbf{n}	\mathbf{n}	\mathbf{n}^*	$e^{\frac{2\pi i}{3}}\mathbf{n}$	$-\mathbf{n}^*$

ing three valley-type and three spin-type flux operators:

$$\Phi_{+;1,2,3}^\dagger = \frac{1}{2}f_{+;s,v}^\dagger [(i\sigma_2)_{ss'} (i\mu_2\mu_{1,2,3})_{vv'}] f_{+;s',v'}^\dagger \widetilde{\mathcal{M}}_+^\dagger, \quad (137)$$

$$\Phi_{+;4,5,6}^\dagger = \frac{i}{2}f_{+;s,v}^\dagger [(i\sigma_2\sigma_{1,2,3})_{ss'} (i\mu_2)_{vv'}] f_{+;s',v'}^\dagger \widetilde{\mathcal{M}}_+^\dagger, \quad (138)$$

where the global phases are chosen to reproduce the flux operators introduced in [31]. We focus on spin-type flux operator for which we introduce the following short-hand notation

$$(\Phi_{+;4}^\dagger, \Phi_{+;5}^\dagger, \Phi_{+;6}^\dagger) \equiv \Phi_{+;S}^\dagger \equiv \mathbf{F}_{+;S}^\dagger \widetilde{\mathcal{M}}_+^\dagger. \quad (139)$$

The flux operator with spin down quantum number is

$$\frac{1}{2}(\Phi_{+;4}^\dagger - i\Phi_{+;5}^\dagger) = if_{+;\downarrow,-\mathbf{Q}}^\dagger f_{+;\downarrow,\mathbf{Q}}^\dagger \widetilde{\mathcal{M}}_+^\dagger. \quad (140)$$

We define monopole operators, similar to Ref. [83], as combinations of flux creation operators and anti-flux destruction operators, e.g. spin-type monopole operators are given by

$$\begin{aligned} \mathcal{S}^\dagger &\equiv (\mathcal{S}_1^\dagger, \mathcal{S}_2^\dagger, \mathcal{S}_3^\dagger) \\ &= (\Phi_{+;4}^\dagger + \Phi_{-;4}, \Phi_{+;5}^\dagger + \Phi_{-;5}, \Phi_{+;6}^\dagger + \Phi_{-;6}). \end{aligned} \quad (141)$$

The transformations properties of these operators are obtained as follows. The transformation properties of the zero modes creation operators $\mathbf{F}_{+;S}^\dagger$ can be found using Tab. V. As for the bare monopole $\widetilde{\mathcal{M}}_+^\dagger$, its transformations are partially constrained by symmetries and the requirement that flux operators Φ_+^\dagger and anti-flux operators Φ_-^\dagger transform between themselves. This does not completely fix $U(1)_{\text{top}}$ phases which were determined numerically in Refs. [19; 31] and analytically [82]. From these transformations, one can then find how flux operators and monopole operators transform under symmetries. The transformation properties of all the operators

mentioned above are shown in Tab. VII. The definition of spin-type monopole operators was chosen (141) such that these operators are odd under time reversal. Note that the C_6 transformation induces an additional phase common to all the monopole operators which can be dropped. By comparing Tab. VI and Tab. VII, we see that the spin

Table VII: Transformation properties under Kagome lattice symmetries and time reversal of a bare monopole $\widetilde{\mathcal{M}}_+^\dagger$, of a spin-type combination of zero modes creation operators $\mathbf{F}_{+;S}^\dagger$ and the corresponding flux operators $\Phi_{+;S}^\dagger$ and monopole operators \mathcal{S}^\dagger .

	$T_{\mathbf{a}_1}$	$T_{\mathbf{a}_2}$	R_y	C_6	\mathcal{T}
$\mathbf{F}_{+;S}^\dagger \rightarrow$	$\mathbf{F}_{+;S}^\dagger$	$\mathbf{F}_{+;S}^\dagger$	$-\mathbf{F}_{-;S}^\dagger$	$\mathbf{F}_{+;S}^\dagger$	$\mathbf{F}_{-;S}^\dagger$
$\widetilde{\mathcal{M}}_+^\dagger \rightarrow$	$\widetilde{\mathcal{M}}_+^\dagger$	$\widetilde{\mathcal{M}}_+^\dagger$	$\widetilde{\mathcal{M}}_-^\dagger$	$e^{\frac{2\pi i}{3}}\widetilde{\mathcal{M}}_+^\dagger$	$-\widetilde{\mathcal{M}}_-^\dagger$
$\Phi_{+;S}^\dagger \rightarrow$	$\Phi_{+;S}^\dagger$	$\Phi_{+;S}^\dagger$	$-\Phi_{-;S}^\dagger$	$e^{\frac{2\pi i}{3}}\Phi_{+;S}^\dagger$	$-\Phi_{-;S}^\dagger$
$\mathcal{S}^\dagger \rightarrow$	\mathcal{S}^\dagger	\mathcal{S}^\dagger	\mathcal{S}	$e^{\frac{2\pi i}{3}}\mathcal{S}^\dagger$	$-\mathcal{S}$

triplet monopole \mathcal{S}^\dagger is the right operator to produce the $\mathbf{q} = 0$ AFM order.

C. Quantum phase transition

The confinement-deconfinement mechanism introduced earlier is thus appropriate to describe the transition from the DSL to the $\mathbf{q} = 0$ coplanar AFM on the Kagome lattice. Following the condensation of a spin-Hall mass driven by the cHGN interaction, spin-type monopole operators proliferate [30] and condense the AFM order. In terms of lattice operators, the spin-Hall bilinear $\bar{\Psi}\sigma\Psi$, or equivalently the auxiliary boson ϕ , corresponds to a vector spin chirality $V^a \sim \sum_{\langle ij \rangle \in \square} (\vec{S}_i \times \vec{S}_j)^a$ [19], where \square denotes an hexagonal plaquette on the Kagome lattice. In this language, the transition is driven by the second neighbor antiferromagnetic interaction which condenses the vector spin chirality, which in turn allows the monopole operators to proliferate on the lattice.

We have just seen that lattice quantum numbers are important to identify the spin down monopole operator as the right operator to induce the AFM. They also determine which combinations of monopole operators transform trivially under all the symmetries of the DSL and thus constitute allowed perturbations in this phase. By inspection of Tab. VII, the sextupled spin down monopole operator, $\mathcal{O} = (\mathcal{S}_1^\dagger - i\mathcal{S}_2^\dagger)^6 + \text{h.c.}$

is identified as a symmetry-allowed perturbation. This is reminiscent of the role that n -tupled monopole operators play for the Neel-VBS transition described by CP^{N_b-1} bosonic theory [20; 51; 84; 85]. The perturbation $\mathcal{O}' = \mathcal{S}_1^\dagger \mathcal{S}_2 + \text{h. c.}$ also respects the symmetries of the Kagome lattice. Among those symmetric perturbations built from spin down monopole operators \mathcal{O}_S , the one with the lowest scaling dimension $\Delta_{\mathcal{O}_S}$ controls the scale ξ_S of the AFM order. The spin-spin connected correlation function is controlled by this length scale ξ_S and the scaling dimension Δ_q of the spin down monopole operator (see Tab. I), scaling as $\langle \mathbf{n}(\mathbf{r}) \cdot \mathbf{n}^\dagger(0) \rangle_c \sim 1/r^{2\Delta_q}$ for $r \ll \xi_S$.

Determining the scaling dimension of these monopole perturbations \mathcal{O}_S for $2N_f = 4$ is important, as the quantum phase transition works out very differently whether these operators are relevant at the QCP or not [86]. If all allowed monopole perturbations \mathcal{O}_S turn out irrelevant at the QCP — as is the case for all monopole operators in the large- N_f limit — then these perturbations are dangerously irrelevant, and monopole operators only proliferate once the spin-Hall mass is condensed. Said otherwise, the QCP is a simple fixed point with one relevant direction being controlled by the boson mass m_ϕ^2 . The length scale ξ controlling the spin-Hall mass condensation is then determined by the critical exponent $\nu^{-1} = d - \Delta_\phi$. The vector spin chirality connected correlation function depends on this length scale ξ and on the scaling dimension Δ_V given by $\min(\Delta_\phi, \Delta_{\bar{\Psi}\sigma_a\Psi})$ (see Tab. IV) at leading order in the loop-expansion [18], scaling as $\langle \mathbf{V}(\mathbf{r}) \cdot \mathbf{V}(0) \rangle_c \sim 1/r^{2\Delta_V}$ for $r \ll \xi$. In this case where the monopole perturbation is a dangerously irrelevant operator, the two length scales ξ_S and ξ are interdependent [18]. At intermediate scales $\xi \ll L \ll \xi_S$, the system is described by a spin liquid where the spinons are gapped since a spin-Hall mass is condensed. At longer scale $L \gg \xi_S$, the spinons are confined and the system is well described by the AFM phase.

VIII. CONCLUSION

We have computed the scaling dimension of monopole operators at the QCP of a confinement-deconfinement transition between a DSL and an AFM phase in the large N_f expansion where $2N_f$ is the number of fermion flavors. We find that the lowest scaling dimension of monopole operators at the QCP is always smaller than at the QED₃ point. For the minimal magnetic charge, this scaling dimension is $\Delta_{q=1/2} = (2N_f)0.19539 + \mathcal{O}(N_f^0)$. We have

considered other possible fermion “zero” modes dressings and found a hierarchy in the scaling dimension of different monopole operators. We also computed the lowest scaling dimension and the range of the monopole operators scaling dimensions using a large q limit. In contrast, the case of the transition to a chiral spin liquid, where a $SU(2N_f)$ symmetric mass is condensed, was shown to have the same leading order scaling dimension as QED₃. To complement our large N_f analysis, we also studied the RG flow of QED₃ with a spin-dependent Yukawa coupling. We found the existence of the QCP and computed critical exponents at one loop using the $d = 4 - \epsilon$ expansion. We characterized the QCP in the case of a Kagome quantum magnet.

We mainly focused on the transition from a DSL to an antiferromagnet and oriented our analysis towards its description. However, the results we obtained for the monopole scaling dimension would be the same with the introduction of a valley-dependent interaction $(\bar{\Psi}\mu\Psi)^2$. We could do a similar development to obtain the scaling dimension of monopole operators. By performing a large N expansion with N the number of spin components, the same scaling dimensions are found. Now, the monopole operator with the lowest scaling dimension is the monopole in the valley triplet with eigenvalue -1 under μ_z . The results at leading order $1/N_f$ is also unchanged whether we pick the $SU(2)_{\text{spin}}$ symmetric interaction $(\bar{\Psi}\sigma\Psi)^2$ or an $SU(2)_{\text{spin}}$ symmetry breaking interaction like $(\bar{\Psi}\sigma_z\Psi)^2$. A similar adaptation can be made for a mixed spin-valley interaction like $(\bar{\Psi}\mu_z\sigma_z\Psi)^2$. In this case, the scaling dimension is also the same at leading order. It would also be interesting to extend the computation and obtain $\mathcal{O}(N_f^0)$ corrections using the same methods as in Refs. [39; 40].

Acknowledgments

We thank Yin-Chen He, Joseph Maciejko, Subir Sachdev, Sergueï Tchoumakov and Chong Wang for useful discussions. ÉD was funded by an Alexander Graham Bell CGS from NSERC. MP was funded by a Discovery Grant from NSERC. WWK was funded by a Discovery Grant from NSERC, a Canada Research Chair, and a “Établissement de nouveaux chercheurs et de nouvelles chercheuses universitaires” grant from FRQNT.

Note added—Shortly after this work was submitted, we became aware of Ref. 87, which partially overlaps with our work.

¹ W. X. Gang, *Quantum field theory of many-body systems: from the origin of sound to an origin of light and electrons* (Oxford University Press, Oxford, 2007).

² L. Balents, *Nature* **464**, 199 EP (2010), URL [https://](https://doi.org/10.1038/nature08917)

doi.org/10.1038/nature08917.

³ Y. Zhou, K. Kanoda, and T.-K. Ng, *Rev. Mod. Phys.* **89**, 025003 (2017), URL <https://link.aps.org/doi/10.1103/RevModPhys.89.025003>.

- ⁴ W. Witczak-Krempa, G. Chen, Y. B. Kim, and L. Balents, Annual Review of Condensed Matter Physics **5**, 57 (2014), <https://doi.org/10.1146/annurev-conmatphys-020911-125138>, URL <https://doi.org/10.1146/annurev-conmatphys-020911-125138>.
- ⁵ M. R. Norman, Rev. Mod. Phys. **88**, 041002 (2016), URL <https://link.aps.org/doi/10.1103/RevModPhys.88.041002>.
- ⁶ L. Savary and L. Balents, Reports on Progress in Physics **80**, 016502 (2016), URL <https://doi.org/10.1088/2F0034-4885/2F80/2F1/2F016502>.
- ⁷ H. Takagi, T. Takayama, G. Jackeli, G. Khaliullin, and S. E. Nagler (2019), arXiv:1903.08081.
- ⁸ A. M. Polyakov, Nuclear Physics B **120**, 429 (1977), ISSN 0550-3213, URL <http://www.sciencedirect.com/science/article/pii/0550321377900864>.
- ⁹ V. Borokhov, A. Kapustin, and X. Wu, Journal of High Energy Physics **2002**, 049 (2003).
- ¹⁰ R. Kaneko, S. Morita, and M. Imada, Journal of the Physical Society of Japan **83**, 093707 (2014), <https://doi.org/10.7566/JPSJ.83.093707>, URL <https://doi.org/10.7566/JPSJ.83.093707>.
- ¹¹ Y. Iqbal, W.-J. Hu, R. Thomale, D. Poilblanc, and F. Becca, Phys. Rev. B **93**, 144411 (2016), URL <https://link.aps.org/doi/10.1103/PhysRevB.93.144411>.
- ¹² Y. Ran, M. Hermele, P. A. Lee, and X.-G. Wen, Physical Review Letters **98** (2007), ISSN 0031-9007, 1079-7114, URL <https://link.aps.org/doi/10.1103/PhysRevLett.98.117205>.
- ¹³ Y. Iqbal, F. Becca, and D. Poilblanc, Phys. Rev. B **84**, 020407 (2011), URL <https://link.aps.org/doi/10.1103/PhysRevB.84.020407>.
- ¹⁴ Y. Iqbal, F. Becca, S. Sorella, and D. Poilblanc, Physical Review B **87** (2013), ISSN 1098-0121, 1550-235X, URL <https://link.aps.org/doi/10.1103/PhysRevB.87.060405>.
- ¹⁵ Y. Iqbal, D. Poilblanc, and F. Becca, Phys. Rev. B **91**, 020402 (2015), URL <https://link.aps.org/doi/10.1103/PhysRevB.91.020402>.
- ¹⁶ Y.-C. He, M. P. Zaletel, M. Oshikawa, and F. Pollmann, Physical Review X **7** (2017), ISSN 2160-3308, URL <https://link.aps.org/doi/10.1103/PhysRevX.7.031020>.
- ¹⁷ H. Liao, Z. Xie, J. Chen, Z. Liu, H. Xie, R. Huang, B. Normand, and T. Xiang, Physical Review Letters **118** (2017), ISSN 0031-9007, 1079-7114, URL <https://link.aps.org/doi/10.1103/PhysRevLett.118.137202>.
- ¹⁸ P. Ghaemi and T. Senthil, Phys. Rev. B **73**, 054415 (2006), URL <https://link.aps.org/doi/10.1103/PhysRevB.73.054415>.
- ¹⁹ M. Hermele, Y. Ran, P. A. Lee, and X.-G. Wen, Physical Review B **77** (2008), ISSN 1098-0121, 1550-235X, arXiv:0803.1150, URL <http://arxiv.org/abs/0803.1150>.
- ²⁰ T. Senthil, L. Balents, S. Sachdev, A. Vishwanath, and M. P. A. Fisher, Phys. Rev. B **70**, 144407 (2004), URL <https://link.aps.org/doi/10.1103/PhysRevB.70.144407>.
- ²¹ C. Wang, A. Nahum, M. A. Metlitski, C. Xu, and T. Senthil, Phys. Rev. X **7**, 031051 (2017), URL <https://link.aps.org/doi/10.1103/PhysRevX.7.031051>.
- ²² M. S. Block, R. G. Melko, and R. K. Kaul, Phys. Rev. Lett. **111**, 137202 (2013), URL <https://link.aps.org/doi/10.1103/PhysRevLett.111.137202>.
- ²³ G. J. Sreejith and S. Powell, Phys. Rev. B **92**, 184413 (2015), URL <https://link.aps.org/doi/10.1103/PhysRevB.92.184413>.
- ²⁴ S. Pujari, F. Alet, and K. Damle, Phys. Rev. B **91**, 104411 (2015), URL <https://link.aps.org/doi/10.1103/PhysRevB.91.104411>.
- ²⁵ M. E. Peskin, Annals of Physics **113**, 122 (1978), ISSN 0003-4916, URL <http://www.sciencedirect.com/science/article/pii/000349167890252X>.
- ²⁶ C. Dasgupta and B. I. Halperin, Phys. Rev. Lett. **47**, 1556 (1981), URL <https://link.aps.org/doi/10.1103/PhysRevLett.47.1556>.
- ²⁷ D. T. Son, Phys. Rev. X **5**, 031027 (2015), URL <https://link.aps.org/doi/10.1103/PhysRevX.5.031027>.
- ²⁸ N. Seiberg, T. Senthil, C. Wang, and E. Witten, Annals of Physics **374**, 395 (2016), ISSN 0003-4916, URL <http://www.sciencedirect.com/science/article/pii/S0003491616301531>.
- ²⁹ A. Karch and D. Tong, Phys. Rev. X **6**, 031043 (2016), URL <https://link.aps.org/doi/10.1103/PhysRevX.6.031043>.
- ³⁰ Y.-M. Lu, G. Y. Cho, and A. Vishwanath, Phys. Rev. B **96**, 205150 (2017), URL <https://link.aps.org/doi/10.1103/PhysRevB.96.205150>.
- ³¹ X.-Y. Song, C. Wang, A. Vishwanath, and Y.-C. He, arXiv:1811.11186 [cond-mat, physics:hep-lat, physics:hep-th] (2018), arXiv: 1811.11186, URL <http://arxiv.org/abs/1811.11186>.
- ³² M. F. Atiyah and I. M. Singer, Bulletin of the American Mathematical Society **69**, 422 (1963), ISSN 0002-9904, 1936-881X, URL <https://www.ams.org/home/page/>.
- ³³ A. M. Polyakov, Physics Letters B **59**, 82 (1975), ISSN 0370-2693, URL <http://www.sciencedirect.com/science/article/pii/0370269375901628>.
- ³⁴ M. Hermele, T. Senthil, M. P. A. Fisher, P. A. Lee, N. Nagaosa, and X.-G. Wen, Phys. Rev. B **70**, 214437 (2004), URL <https://link.aps.org/doi/10.1103/PhysRevB.70.214437>.
- ³⁵ X. Y. Xu, Y. Qi, L. Zhang, F. F. Assaad, C. Xu, and Z. Y. Meng (2018), arXiv:1807.07574.
- ³⁶ S. Rychkov, *EPFL Lectures on Conformal Field Theory in D = 3 Dimensions*, SpringerBriefs in Physics (Springer International Publishing, 2017), ISBN 978-3-319-43625-8, URL <http://www.springer.com/gp/book/9783319436258>.
- ³⁷ E. Dyer, M. Mezei, and S. S. Pufu, arXiv:1309.1160 [cond-mat, physics:hep-th] (2013), arXiv: 1309.1160, URL <http://arxiv.org/abs/1309.1160>.
- ³⁸ M. A. Metlitski, M. Hermele, T. Senthil, and M. P. A. Fisher, Physical Review B **78** (2008), ISSN 1098-0121, 1550-235X, URL <https://link.aps.org/doi/10.1103/PhysRevB.78.214418>.
- ³⁹ S. S. Pufu, Physical Review D **89** (2014), ISSN 1550-7998, 1550-2368, URL <https://link.aps.org/doi/10.1103/PhysRevD.89.065016>.
- ⁴⁰ E. Dyer, M. Mezei, S. S. Pufu, and S. Sachdev, Journal of High Energy Physics **2015** (2015), ISSN 1029-8479, URL [http://link.springer.com/10.1007/JHEP06\(2015\)037](http://link.springer.com/10.1007/JHEP06(2015)037).
- ⁴¹ S. S. Pufu and S. Sachdev, Journal of High Energy Physics **2013** (2013), ISSN 1029-8479, URL [http://link.springer.com/10.1007/JHEP09\(2013\)127](http://link.springer.com/10.1007/JHEP09(2013)127).
- ⁴² V. Borokhov, A. Kapustin, and X. Wu, Journal of High Energy Physics **2002**, 044 (2002), ISSN 1029-8479, URL <http://stacks.iop.org/1126-6708/2002/i=12/a=044?key=crossref.62e8903454b6a90cca5db93bdc6fbd62>.
- ⁴³ Đ. Radicević, Journal of High Energy Physics **2016**, 131 (2016), ISSN 1029-8479, URL [https://doi.org/10.1007/1007/JHEP09\(2013\)127](https://doi.org/10.1007/1007/JHEP09(2013)127).

- JHEP03(2016)131.
- ⁴⁴ S. M. Chester, L. V. Iliesiu, M. Mezei, and S. S. Pufu, *Journal of High Energy Physics* **2018** (2018), ISSN 1029-8479, URL [http://link.springer.com/10.1007/JHEP05\(2018\)157](http://link.springer.com/10.1007/JHEP05(2018)157).
 - ⁴⁵ S. Weinberg, *The quantum theory of fields. Vol. 3: Supersymmetry* (Cambridge University Press, 2013), ISBN 9780521670555, 9781139632638, 9780521670555.
 - ⁴⁶ T. T. Wu and C. N. Yang, *Nuclear Physics B* **107**, 365 (1976).
 - ⁴⁷ DLMF, *NIST Digital Library of Mathematical Functions*, <http://dlmf.nist.gov/>, Release 1.0.21 of 2018-12-15, f. W. J. Olver, A. B. Olde Daalhuis, D. W. Lozier, B. I. Schneider, R. F. Boisvert, C. W. Clark, B. R. Miller and B. V. Saunders, eds., URL <http://dlmf.nist.gov/>.
 - ⁴⁸ S. Hellerman, D. Orlando, S. Reffert, and M. Watanabe, *Journal of High Energy Physics* **2015**, 1 (2015), ISSN 1029-8479, URL [https://doi.org/10.1007/JHEP12\(2015\)071](https://doi.org/10.1007/JHEP12(2015)071).
 - ⁴⁹ A. de la Fuente, *Journal of High Energy Physics* **2018**, 41 (2018), ISSN 1029-8479, URL [https://doi.org/10.1007/JHEP08\(2018\)041](https://doi.org/10.1007/JHEP08(2018)041).
 - ⁵⁰ R. Boyack, C.-H. Lin, N. Zerf, A. Rayyan, and J. Maciejko, *Phys. Rev. B* **98**, 035137 (2018), URL <https://link.aps.org/doi/10.1103/PhysRevB.98.035137>.
 - ⁵¹ M. A. Metlitski and R. Thorngren, *Phys. Rev. B* **98**, 085140 (2018), URL <https://link.aps.org/doi/10.1103/PhysRevB.98.085140>.
 - ⁵² L. Bartosch, *Phys. Rev. B* **88**, 195140 (2013), URL <https://link.aps.org/doi/10.1103/PhysRevB.88.195140>.
 - ⁵³ A. W. Sandvik, *Phys. Rev. Lett.* **98**, 227202 (2007), URL <https://link.aps.org/doi/10.1103/PhysRevLett.98.227202>.
 - ⁵⁴ R. G. Melko and R. K. Kaul, *Phys. Rev. Lett.* **100**, 017203 (2008), URL <https://link.aps.org/doi/10.1103/PhysRevLett.100.017203>.
 - ⁵⁵ R. K. Kaul and A. W. Sandvik, *Phys. Rev. Lett.* **108**, 137201 (2012), URL <https://link.aps.org/doi/10.1103/PhysRevLett.108.137201>.
 - ⁵⁶ S. Pujari, K. Damle, and F. Alet, *Phys. Rev. Lett.* **111**, 087203 (2013), URL <https://link.aps.org/doi/10.1103/PhysRevLett.111.087203>.
 - ⁵⁷ A. Nahum, J. T. Chalker, P. Serna, M. Ortuño, and A. M. Somoza, *Phys. Rev. X* **5**, 041048 (2015), URL <https://link.aps.org/doi/10.1103/PhysRevX.5.041048>.
 - ⁵⁸ R. Boyack, A. Rayyan, and J. Maciejko (2018), URL <https://arxiv.org/abs/1812.02720v1>.
 - ⁵⁹ N. Zerf, L. N. Mihaila, P. Marquard, I. F. Herbut, and M. M. Scherer, *Phys. Rev. D* **96**, 096010 (2017), URL <https://link.aps.org/doi/10.1103/PhysRevD.96.096010>.
 - ⁶⁰ J. A. Gracey, *Phys. Rev. D* **97**, 105009 (2018), URL <https://link.aps.org/doi/10.1103/PhysRevD.97.105009>.
 - ⁶¹ L. Janssen and Y.-C. He, *Phys. Rev. B* **96**, 205113 (2017), URL <https://link.aps.org/doi/10.1103/PhysRevB.96.205113>.
 - ⁶² B. Ihrig, L. Janssen, L. N. Mihaila, and M. M. Scherer, *Phys. Rev. B* **98**, 115163 (2018), URL <https://link.aps.org/doi/10.1103/PhysRevB.98.115163>.
 - ⁶³ N. Zerf, P. Marquard, R. Boyack, and J. Maciejko, *Phys. Rev. B* **98**, 165125 (2018), URL <https://link.aps.org/doi/10.1103/PhysRevB.98.165125>.
 - ⁶⁴ J. A. Gracey, *Phys. Rev. D* **98**, 085012 (2018), URL <https://link.aps.org/doi/10.1103/PhysRevD.98.085012>.
 - ⁶⁵ S. Benvenuti and H. Khachatryan (2019), URL <https://arxiv.org/abs/1902.05767v1>.
 - ⁶⁶ J. A. Gracey, *International Journal of Modern Physics A* **33**, 1830032 (2018).
 - ⁶⁷ S. Sachdev, *Quantum Phase Transitions* (Cambridge University Press, 2011), ISBN 9781139500210.
 - ⁶⁸ L. Iliesiu, F. Kos, D. Poland, S. S. Pufu, D. Simmons-Duffin, and R. Yacoby, *Journal of High Energy Physics* **2016**, 120 (2016), ISSN 1029-8479, URL [https://doi.org/10.1007/JHEP03\(2016\)120](https://doi.org/10.1007/JHEP03(2016)120).
 - ⁶⁹ G. Tarnopolsky, L. Fei, S. Giombi, and I. R. Klebanov, *Progress of Theoretical and Experimental Physics* **2016** (2016), ISSN 2050-3911, URL <https://dx.doi.org/10.1093/ptep/ptw120>.
 - ⁷⁰ M. P. Shores, E. A. Nytko, B. M. Bartlett, and D. G. Nocera, *Journal of the American Chemical Society* **127**, 13462 (2005), ISSN 0002-7863, URL <https://doi.org/10.1021/ja053891p>.
 - ⁷¹ P. Sindzingre and C. Lhuillier, *EPL (Europhysics Letters)* **88**, 27009 (2009), ISSN 0295-5075, 1286-4854, URL <http://stacks.iop.org/0295-5075/88/i=2/a=27009?key=crossref.752c93f247677a2b76a9147453e6f80d>.
 - ⁷² W. Zhu, X. Chen, Y.-C. He, and W. Witczak-Krempa, *Science Advances* **4** (2018), URL <https://advances.sciencemag.org/content/4/11/eaat5535>.
 - ⁷³ H. C. Jiang, Z. Y. Weng, and D. N. Sheng, *Physical Review Letters* **101** (2008), ISSN 0031-9007, 1079-7114, URL <https://link.aps.org/doi/10.1103/PhysRevLett.101.117203>.
 - ⁷⁴ O. Gtze, D. J. J. Farnell, R. F. Bishop, P. H. Y. Li, and J. Richter, *Physical Review B* **84** (2011), ISSN 1098-0121, 1550-235X, URL <https://link.aps.org/doi/10.1103/PhysRevB.84.224428>.
 - ⁷⁵ S. Yan, D. A. Huse, and S. R. White, *Science* **332**, 1173 (2011), ISSN 0036-8075, 1095-9203, URL <http://science.sciencemag.org/content/332/6034/1173>.
 - ⁷⁶ H.-C. Jiang, Z. Wang, and L. Balents, *Nature Physics* **8**, 902 EP (2012), article, URL <https://doi.org/10.1038/nphys2465>.
 - ⁷⁷ S. Depenbrock, I. P. McCulloch, and U. Schollwöck, *Physical Review Letters* **109** (2012), ISSN 0031-9007, 1079-7114, URL <https://link.aps.org/doi/10.1103/PhysRevLett.109.067201>.
 - ⁷⁸ J.-W. Mei, J.-Y. Chen, H. He, and X.-G. Wen, *Physical Review B* **95** (2017), ISSN 2469-9950, 2469-9969, URL <https://link.aps.org/doi/10.1103/PhysRevB.95.235107>.
 - ⁷⁹ M. B. Hastings, *Phys. Rev. B* **63**, 014413 (2000), URL <https://link.aps.org/doi/10.1103/PhysRevB.63.014413>.
 - ⁸⁰ S.-S. Gong, W. Zhu, L. Balents, and D. N. Sheng, *Phys. Rev. B* **91**, 075112 (2015), URL <https://link.aps.org/doi/10.1103/PhysRevB.91.075112>.
 - ⁸¹ F. Kolley, S. Depenbrock, I. P. McCulloch, U. Schollwöck, and V. Alba, *Phys. Rev. B* **91**, 104418 (2015), URL <https://link.aps.org/doi/10.1103/PhysRevB.91.104418>.
 - ⁸² X.-Y. Song, Y.-C. He, A. Vishwanath, and C. Wang, *arXiv:1811.11182 [cond-mat, physics:hep-lat, physics:hep-th]* (2018), arXiv: 1811.11182, URL <http://arxiv.org/abs/1811.11182>.
 - ⁸³ J. Alicea, *Physical Review B* **78** (2008), ISSN 1098-0121, 1550-235X, URL <https://link.aps.org/doi/10.1103/PhysRevB.78.035126>.
 - ⁸⁴ N. Read and S. Sachdev, *Phys. Rev. B* **42**, 4568 (1990), URL <https://link.aps.org/doi/10.1103/PhysRevB.42.4568>.

- ⁸⁵ J. Lee and S. Sachdev, Phys. Rev. Lett. **114**, 226801 (2015), URL <https://link.aps.org/doi/10.1103/PhysRevLett.114.226801>.
⁸⁶ J. Y. Lee, Y.-Z. You, S. Sachdev, and A. Vishwanath,

- arXiv e-prints arXiv:1904.07266 (2019), 1904.07266.
⁸⁷ N. Zerf, R. Boyack, P. Marquard, J. A. Gracey, and J. Maciejko (2019), arXiv:1905.03719.

Appendix A: Regularization of the integrated logarithm

The divergent integral $\int d\omega \log(\omega^2 + a^2)$ can be rewritten by using $\log A = -dA^{-s}/ds|_{s=0}$. The resulting expression integrates to an hyper-geometric function

$$\int_{-\infty}^{\infty} d\omega \log(\omega^2 + a^2) = -\frac{d}{ds} \int d\omega (\omega^2 + a^2)^{-s} \Big|_{s=0} = 2 \left(-\frac{d}{ds} a^{1-2s} \left[\omega {}_2F_1 \left(\frac{1}{2}, s; \frac{3}{2}; -\omega^2 \right) \right]_{\omega=\infty} \Big|_{s=0} \right), \quad (\text{A1})$$

where it was assumed that $a > 0$, which is the case in the main text where $a = \{M_q, \varepsilon_\ell\}$. The analytic continuation then yields

$$\int_{-\infty}^{\infty} d\omega \log(\omega^2 + a^2) = 2 \left(-\frac{d}{ds} a^{1-2s} \left(\frac{\sqrt{\pi} \Gamma(-s - \frac{1}{2})}{2\Gamma(-s)} \right) \Big|_{s=0} \right) = 2 \left(-a \frac{d}{ds} (-\pi s + O(s^2)) \Big|_{s=0} \right) = 2\pi a. \quad (\text{A2})$$

Alternatively, we can also regularize this integral by introducing a frequency UV cut-off Λ and by keeping only the finite part as it is taken to infinity

$$\int_{-\Lambda}^{\Lambda} d\omega \log(\omega^2 + a^2) = 4\Lambda (\log(\Lambda) - 1) + 2\pi a + \mathcal{O}(\Lambda^{-1}) \rightarrow 2\pi a. \quad (\text{A3})$$

Appendix B: Saddle point equations for QED₃ – cHGN in a thermal setup

In Sec. III, we obtained the lowest scaling dimension Δ_q of monopole operators in QED₃ – cHGN. We did this by computing the leading order free energy $F_q^{(0)}$ (19) on $S^2 \times \mathbb{R}$ with appropriate magnetic flux. We saw that in the case of a SU(2N_f) symmetric interaction, the computation should be performed on a compactified “time” direction $\mathbb{R} \rightarrow S^1_\beta$. Here, we repeat the computation in the former theory now using the “thermal” setup,

$$F_q^{(0)} = -\frac{1}{\beta} \log \det [\not{D}_{-i\mu, A^q} + M_q \sigma_z] \quad (\text{B1})$$

$$= -\frac{1}{\beta} \sum_{\sigma=\pm 1} \sum_{n \in \mathbb{Z}} \left[d_q \log [\omega_n - i\mu + i\sigma M_q] + \sum_{\ell=q+1}^{\infty} d_\ell \log [(\omega_n - i\mu)^2 + \varepsilon_\ell^2] \right], \quad (\text{B2})$$

where as before ε_ℓ is given by Eq.(32) and ω_n are the Matsubara frequencies. First taking the sum over the magnetic spin degrees of freedom and then regularizing the sum on Matsubara frequencies, this expression becomes

$$F_q^{(0)} = -\frac{1}{\beta} \sum_{n \in \mathbb{Z}} \left[d_q \log [(\omega_n - i\mu)^2 + M_q^2] + \sum_{\ell=q+1}^{\infty} 2d_\ell \log [(\omega_n - i\mu)^2 + \varepsilon_\ell^2] \right] \quad (\text{B3})$$

$$= -\frac{1}{\beta} \left[d_q \log [2 (\cosh(\beta M_q) + \cosh(\beta \mu))] + \sum_{\ell=q+1}^{\infty} 2d_\ell \log [2 (\cosh(\beta \varepsilon_\ell) + \cosh(\beta \mu))] \right]. \quad (\text{B4})$$

The saddle point equations are

$$0 = \frac{\partial F_q^{(0)}}{\partial \mu} = -d_q \left(\frac{\sinh(\beta \mu)}{\cosh(\beta M_q) + \cosh(\beta \mu)} \right) - \sum_{\ell=q+1}^{\infty} 2d_\ell \left(\frac{\sinh(\beta \mu)}{\cosh(\beta \varepsilon_\ell) + \cosh(\beta \mu)} \right), \quad (\text{B5})$$

$$0 = \frac{\partial F_q^{(0)}}{\partial M_q} = -d_q \left(\frac{\sinh(\beta M_q)}{\cosh(\beta M_q) + \cosh(\beta \mu)} \right) - \sum_{\ell=q+1}^{\infty} 2d_\ell \varepsilon_\ell^{-1} M_q \left(\frac{\sinh(\beta \varepsilon_\ell)}{\cosh(\beta \varepsilon_\ell) + \cosh(\beta \mu)} \right). \quad (\text{B6})$$

The first saddle point equation is solved with $\mu = 0$. This is the reason why the formalism used in the present section is unnecessary, as it was mentioned in Sec. V. Setting $\mu = 0$ in the second saddle point equation yields

$$0 = \left. \frac{\partial F_q^{(0)}}{\partial M_q} \right|_{\mu=0} = -d_q \left(\frac{\sinh(\beta M_q)}{1 + \cosh(\beta M_q)} \right) - \sum_{\ell=q+1}^{\infty} 2d_\ell \varepsilon_\ell^{-1} M_q \left(\frac{\sinh(\beta \varepsilon_\ell)}{1 + \cosh(\beta \varepsilon_\ell)} \right). \quad (\text{B7})$$

We get the interesting result that $M_q = 0$ is a solution of this saddle point equation. This solution was not observed by working directly on $S^2 \times \mathbb{R}$. Assuming $M_q > 0$, the saddle point equation at leading order in $1/\beta$ yields the following condition

$$0 = d_q + \sum_{\ell=q+1}^{\infty} 2d_\ell \varepsilon_\ell^{-1} M_q, \quad (\text{B8})$$

A non trivial solution $M_q \neq 0$ can be found numerically as in the main text. We distinguish the trivial and non-trivial solutions by studying the second derivatives of the free energy at these points. The second derivative in the μ direction designates imaginary fluctuations of the gauge field and as such has no physical signification. We only compute the second derivative in the M_q direction

$$\left. \frac{\partial^2 F_q^{(0)}}{\partial M_q^2} \right|_{\mu=0} = -d_q \left(\frac{\beta}{1 + \cosh(\beta M_q)} \right) - \sum_{\ell=q+1}^{\infty} 2d_\ell \left(\frac{(\varepsilon_\ell^2 - M_q^2) \sinh(\beta \varepsilon_\ell) + \beta M_q^2 \varepsilon_\ell}{\varepsilon_\ell^3 (1 + \cosh(\beta \varepsilon_\ell))} \right). \quad (\text{B9})$$

We study the cases $M_q \neq 0$ and $M_q = 0$ separately. We start with the former case. The second derivative at leading order in $1/\beta$ is

$$\left. \frac{\partial^2 F_q^{(0)}}{\partial M_q^2} \right|_{\mu=0, M_q \neq 0} = -2 \sum_{\ell=q+1}^{\infty} \frac{d_\ell (\varepsilon_\ell^2 - M_q^2)}{\varepsilon_\ell^3}. \quad (\text{B10})$$

Using the saddle point condition (B8) obtained for large β , this can be reformulated as

$$\left. \frac{\partial^2 F_q^{(0)}}{\partial M_q^2} \right|_{\mu=0, M_q \neq 0} = d_q \frac{1}{M_q} + 2 \sum_{\ell=q+1}^{\infty} \frac{M_q^2}{\varepsilon_\ell^3} > 0. \quad (\text{B11})$$

The non trivial solution $M_q \neq 0$ thus corresponds to a minimum. The case of a vanishing mass $M_q = 0$ is now studied. In the large β limit, the second derivative of the free energy at leading order in $1/\beta$ is given by

$$\left. \frac{\partial^2 F_q^{(0)}}{\partial M_q^2} \right|_{\mu=0, M_q=0} = -\frac{\beta}{4} < 0. \quad (\text{B12})$$

Thus, when setting $\mu = 0$, $M_q = 0$ is a maximum.

Appendix C: Feynman diagrams computation

A RG study of the QED₃ – cHGNy model was shown in Sec.VI. In the present section, we compute the one-loop corrections to the wavefunction normalization and coupling constants of this QFT necessary to obtain the RG flow equations shown in the main text.

1. Feynman rules

We first write down the Feynman rules of the QED₃ – cHGNy field theory defined by the lagrangian (72)

$$\overrightarrow{sv} \xrightarrow[p]{s'v'} = G_{sv;s'v'}(p) \equiv \langle \psi_{sv}(p) \bar{\psi}_{s'v'}(p) \rangle = \delta_{ss'} \delta_{vv'} \frac{\not{p}}{p^2}, \quad (C1)$$

$$\overrightarrow{a} \cdots \overrightarrow{b} \xrightarrow[p]{p} = D_{ab}(p) \equiv \langle \phi_a(p) \phi_b(-p) \rangle = \frac{\delta_{ab}}{p^2}, \quad (C2)$$

$$\overrightarrow{\mu} \text{ wavy } \overrightarrow{\nu} \xrightarrow[p]{p} = \Pi_{\mu\nu}(p) \equiv \langle a_\mu(p) a_\nu(-p) \rangle = \frac{1}{p^2} \left(\delta_{\mu\nu} + (\xi - 1) \frac{p_\mu p_\nu}{p^2} \right), \quad (C3)$$

$$\begin{array}{c} \nearrow \\ \nearrow \end{array} \cdots \overrightarrow{a} = h\sigma_a, \quad (C4)$$

$$\begin{array}{c} \nearrow \\ \nearrow \end{array} \text{ wavy } \overrightarrow{\mu} = ie\gamma_\mu, \quad (C5)$$

$$\begin{array}{c} \overrightarrow{a} \quad \overrightarrow{c} \\ \diagdown \quad \diagup \\ \overrightarrow{b} \quad \overrightarrow{d} \end{array} = 8\lambda (\delta_{ab}\delta_{cd} + \delta_{ac}\delta_{bd} + \delta_{ad}\delta_{bc}), \quad (C6)$$

where ξ is the gauge-fixing parameter for the gauge field a_μ . Here, ψ_{sv} is a two-component Dirac spinor with magnetic spin s and valley index v . The mass perturbations can also be treated as interactions with the following Feynman rules

$$\begin{array}{c} \overrightarrow{a} \\ \diagdown \end{array} \times = m_\phi^2 \delta_{ab}, \quad (C7)$$

$$\begin{array}{c} \overrightarrow{b} \\ \diagdown \end{array} \times = m_\psi, \quad (C8)$$

$$\begin{array}{c} \nearrow \\ \nearrow \end{array} \times \overrightarrow{a} = \tilde{m}_\psi \sigma_a. \quad (C9)$$

2. Computation of one-loop Feynman diagrams

We now compute the one-loop Feynman diagrams using the Feynman rules in Sec.C1. First, let us introduce shorthand notation. The diagrams involve a momentum shell loop integral factor \tilde{I}

$$\tilde{I} = \int_{k=\Lambda e^{-l}}^{k=\Lambda} \frac{d^d k}{(2\pi)^d} \frac{1}{k^4} = \left(\frac{\int d\Omega_{d-1}}{(2\pi)^d} \Lambda^{d-4} \right) dl. \quad (C10)$$

The momentum space measure is also abbreviated as $(d\mathbf{k}) \equiv d^d k / (2\pi)^d$. As we write the Feynman diagrams, we identify the corresponding correction to the normalization factors, δZ_{x_i} with $x_i \in \{\psi, \phi, a, e, h, \lambda\}$.

a. Three-point functions

We compute the vertex diagrams shown in Fig. 10

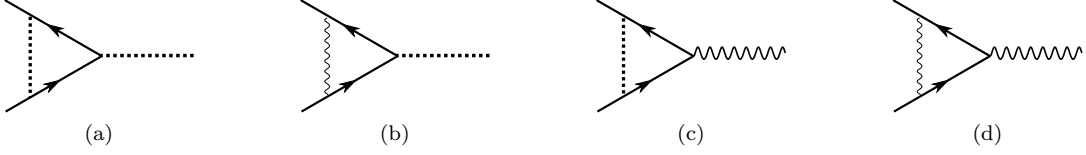


Figure 10: One-loop vertex diagrams.

$$[10(a)] = h\sigma_a \left(\delta Z_h^{(\phi)} \right) = h^3 \int (d\mathbf{k}) \sigma^b G(k) \sigma_a G(k) \sigma^c D_{bc}(k) = h\sigma_a \left(-h^2 (N_b - 2) \tilde{I} \right), \quad (C11)$$

$$[10(b)] = h\sigma_a \left(\delta Z_h^{(a)} \right) = h (ie)^2 \int (d\mathbf{k}) \gamma^\mu G(k) \sigma_a G(k) \gamma^\nu \Pi_{\mu\nu}(k) = h\sigma_a \left(-e^2 (d + \xi - 1) \tilde{I} \right), \quad (C12)$$

$$[10(c)] = ie\gamma^\alpha \left(\delta Z_e^{(\phi)} \right) = ie (-h)^2 \int (d\mathbf{k}) \sigma^b G(k) \gamma^\alpha G(k) \sigma^c D_{bc}(k) = ie\gamma^\alpha \left(-h^2 N_b \left(\frac{d-2}{d} \right) \tilde{I} \right). \quad (C13)$$

The last diagram involves a longer computation

$$\begin{aligned} [10(d)] &= ie\gamma^\alpha \left(\delta Z_e^{(a)} \right) = ie (ie)^2 \int (d\mathbf{k}) \gamma^\mu G(k) \gamma^\alpha G(k) \gamma^\nu \Pi_{\mu\nu}(k) \\ &= ie (ie)^2 \int (d\mathbf{k}) \frac{1}{k^4} \gamma^\mu \gamma^\lambda \gamma^\alpha \gamma^\rho \gamma^\nu \left[\frac{1}{d} \delta^{\mu\nu} \delta^{\lambda\rho} + \left(\frac{\xi - 1}{d(d+2)} \right) (\delta^{\mu\nu} \delta^{\lambda\rho} + \delta^{\mu\lambda} \delta^{\nu\rho} + \delta^{\mu\rho} \delta^{\nu\lambda}) \right] \\ &= ie (ie)^2 \int (d\mathbf{k}) \frac{1}{k^4} \left(\frac{(d-2)^2}{d} \gamma^\alpha + \left(\frac{\xi - 1}{d(d+2)} \right) ((d-2)^2 \gamma^\alpha + d^2 \gamma^\alpha + \gamma^\rho (4\delta^{\alpha\rho} - (4-d) \gamma^\alpha \gamma^\rho)) \right) \\ &= ie\gamma^\alpha \left(-e^2 \left(d - 5 + \frac{4}{d} + \xi \right) \tilde{I} \right), \end{aligned} \quad (C14)$$

where we used gamma identities

$$\gamma^\mu \gamma^\alpha \gamma^\beta \gamma^\mu = 4\delta^{\alpha\beta} - (4-d) \gamma^\alpha \gamma^\beta, \quad (C15)$$

$$\gamma^\mu \gamma^\nu \gamma^\rho \gamma^\lambda \gamma^\mu = -2\gamma^\lambda \gamma^\rho \gamma^\nu + (4-d) \gamma^\nu \gamma^\rho \gamma^\lambda, \quad (C16)$$

and a symmetrization of momentum components appearing in loop integrals,

$$k^\lambda k^\rho \rightarrow \frac{k^2}{d} \delta^{\lambda\rho}, \quad (C17)$$

$$k^\alpha k^\beta k^\gamma k^\delta \rightarrow \frac{k^4}{d(d+2)} (\delta^{\alpha\beta} \delta^{\gamma\delta} + \delta^{\alpha\gamma} \delta^{\beta\delta} + \delta^{\alpha\delta} \delta^{\beta\gamma}). \quad (C18)$$

b. Two-point functions

The two-point diagrams are shown in Fig. 11. The boson contribution to the fermion self-energy is



Figure 11: One-loop two-point diagrams.

$$\begin{aligned}
\delta Z_\psi^{(\phi)} &= -\frac{\partial}{\partial \not{p}}[11(a)] = -(\gamma^\mu)^{-1} \frac{\partial}{\partial p^\mu} \left((h)^2 \int (d\mathbf{k}) \sigma^b G(p-k) \sigma^c D_{bc}(k) \right) \\
&= (\gamma^\mu)^{-1} (h)^2 \int (d\mathbf{k}) \sigma^b G(p-k) \frac{\partial G^{-1}(p-k)}{\partial p^\mu} G(p-k) \sigma^c D_{bc}(k) \\
&= (\gamma^\mu)^{-1} (h)^2 \int (d\mathbf{k}) \sigma^b G(p-k) \gamma^\mu G(p-k) \sigma^c D_{bc}(k) \\
&\stackrel{p \rightarrow 0}{=} \delta Z_e^{(\phi)}.
\end{aligned} \tag{C19}$$

Similarly, the gauge field contribution is related to another vertex correction

$$\delta Z_\psi^{(A)} = -\frac{\partial}{\partial \not{p}}[11(b)] = \delta Z_e^{(A)}. \tag{C20}$$

These results are the one-loop version of the Ward identity. As for the boson ϕ self-energy, it only gets a one-loop contribution by the fermion

$$\begin{aligned}
[11(c)] &= p^2 \delta_{ab} \left(-\delta Z_\phi^{(\psi)} \right) = -(h)^2 \int (d\mathbf{k}) \text{tr} \{ \sigma_a G(k) \sigma_b G(k+p) \} \\
&= -(h)^2 (d_\sigma d_\mu d_\gamma) \delta_{ab} \int (d\mathbf{k}) \frac{k \cdot (k+p)}{k^2 (k+p)^2} \\
&= -(h)^2 (d_\sigma d_\mu d_\gamma) \delta_{ab} \int_0^1 dx \int (d\mathbf{k}) \frac{(k-px) \cdot (k+p(1-x))}{[k^2 + p^2 x(1-x)]^2} \\
&= p^2 \delta_{ab} \left(2N_f h^2 \tilde{I} \right),
\end{aligned} \tag{C21}$$

where d_σ , d_μ and d_γ are the size of the respective SU(2) representations, respectively 2, N_f and 2, and where we introduced a Feynman parameter x . The gauge field also only gets a correction from the fermion

$$\begin{aligned}
[11(d)] &= (p^2 \delta_{\mu\nu} - p_\mu p_\nu / p^2) \left(-\delta Z_a^{(\psi)} \right) = -(ie)^2 \int (d\mathbf{k}) \text{tr} \{ \gamma^\mu G(k) \gamma^\nu G(k+p) \} \\
&= e^2 \int dx \int (d\mathbf{k}) \frac{\text{tr} \{ \gamma^\mu (\not{k} - \not{p}x) \gamma^\nu [(\not{k} + \not{p}(1-x))] \}}{[k^2 + p^2 x(1-x)]^2} \\
&= e^2 \int dx \int (d\mathbf{k}) \frac{\text{tr} \left\{ \frac{(2-d)}{d} k^2 \gamma^\mu \gamma^\nu - x(1-x) p^\alpha p^\beta \gamma^\mu \gamma^\alpha \gamma^\nu \gamma^\beta \right\}}{[k^2 + p^2 x(1-x)]^2} \\
&= 4N_f e^2 \int dx \int (d\mathbf{k}) \frac{\frac{(2-d)}{d} k^2 \delta_{\mu\nu} - x(1-x) p^\alpha p^\beta (\delta^{\mu\alpha} \delta^{\nu\beta} - \delta^{\mu\nu} \delta^{\alpha\beta} + \delta^{\mu\beta} \delta^{\alpha\nu})}{[k^2 + p^2 x(1-x)]^2} \\
&= 4N_f e^2 \int dx \int (d\mathbf{k}) \frac{\delta_{\mu\nu} \left[\frac{(2-d)}{d} k^2 - p^2 \right] + 2x(1-x) (\delta_{\mu\nu} p^2 - p^\mu p^\nu)}{[k^2 + p^2 x(1-x)]^2}.
\end{aligned} \tag{C22}$$

The polarization tensor should be proportional to the transverse tensor $\delta_{\mu\nu} - p_\mu p_\nu / p^2$. This form cannot be achieved with a cut-off regularization which breaks Lorentz invariance. Terms that don't satisfy this form are removed. Since a $p_\mu p_\nu$ term cannot be generated by expansion of the denominator, the $p_\mu p_\nu$ term in the numerator serves as a reference to single out the polarization tensor

$$\begin{aligned}
[11(d)] &= (p^2 \delta_{\mu\nu} - p_\mu p_\nu / p^2) \left(-\delta Z_a^{(\psi)} \right) = (p^2 \delta_{\mu\nu} - p_\mu p_\nu / p^2) \left(4N_f e^2 \left(\int dx 2x(1-x) \right) \tilde{I} \right) \\
&= (p^2 \delta_{\mu\nu} - p_\mu p_\nu / p^2) \left(\frac{4N_f}{3} e^2 \tilde{I} \right).
\end{aligned} \tag{C23}$$

c. Four-point function

The four-point diagrams are shown in Fig. 12.

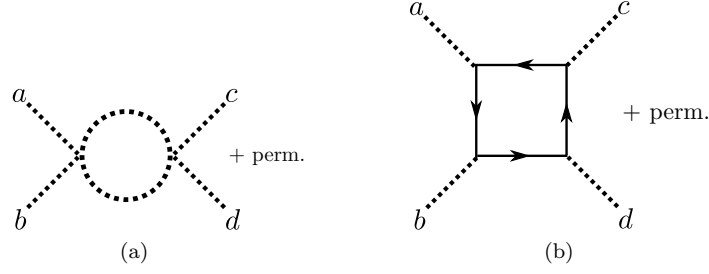


Figure 12: One-loop four-point diagrams.

The boson autointeraction's correction has a contribution from the boson

$$\begin{aligned}
 [12(a)] &= 8\lambda (\delta_{ab}\delta_{cd} + \delta_{ac}\delta_{bd} + \delta_{ad}\delta_{bc}) \left(\delta Z_{\lambda}^{\phi} \right) = \frac{1}{2} [8\lambda (\delta_{ab}\delta_{ef} + \delta_{ae}\delta_{bf} + \delta_{af}\delta_{be})] [8\lambda (\delta_{cd}\delta_{ef} + \delta_{ce}\delta_{df} + \delta_{cf}\delta_{de})] \tilde{I} + \text{perm.} \\
 &= 8\lambda (\delta_{ab}\delta_{cd} + \delta_{ac}\delta_{bd} + \delta_{ad}\delta_{bc}) \left(4(N_b + 8)\lambda \tilde{I} \right), \quad (C24)
 \end{aligned}$$

where the factor $1/2$ is a symmetry factor. The fermion also contributes to the correction

$$\begin{aligned}
 [12(b)] &= 8\lambda (\delta_{ab}\delta_{cd} + \delta_{ac}\delta_{bd} + \delta_{ad}\delta_{bc}) \left(\delta Z_{\lambda}^{\psi} \right) = -h^4 (\text{tr}\{\sigma_a\sigma_b\sigma_c\sigma_d\} + \text{tr}\{\sigma_d\sigma_c\sigma_b\sigma_a\}) \tilde{I} \\
 &= 8\lambda (\delta_{ab}\delta_{cd} + \delta_{ac}\delta_{bd} + \delta_{ad}\delta_{bc}) \left(-h^4\lambda^{-1}N_f\tilde{I} \right). \quad (C25)
 \end{aligned}$$

d. Mass perturbations

Diagrams corresponding to mass perturbation are shown in Fig. 13. Some of the one-loop diagrams for the bilinear

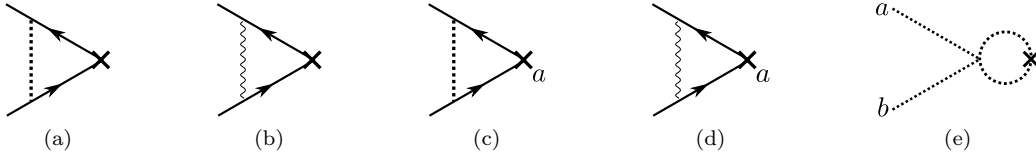


Figure 13: One-loop diagrams corresponding to mass perturbations.

perturbations can be related to previously computed diagrams

$$[13(a)] = m_{\psi} \left(\delta Z_{m_{\psi}}^{(\phi)} \right) = m_{\psi} N_b \frac{1}{((2 - N_b) h \text{tr}\{\mathbb{I}\})} \text{tr}\{\sigma_a[10(a)]_a\} = m_{\psi} \left(N_b h^2 \tilde{I} \right), \quad (C26)$$

$$[13(b)] = m_{\psi} \left(\delta Z_{m_{\psi}}^{(a)} \right) = m_{\psi} \frac{1}{(h \text{tr}\{\mathbb{I}\})} \text{tr}\{\sigma_a[10(b)]_a\} = m_{\psi} \left(-(d + \xi - 1) e^2 \tilde{I} \right), \quad (C27)$$

$$[13(c)] = \tilde{m}_{\psi} \sigma_a \left(\delta Z_{\tilde{m}_{\psi}}^{(\phi)} \right) = \tilde{m}_{\psi} h^{-1} [10(a)]_a = \tilde{m}_{\psi} \sigma_a \left(-(N_b - 2) h^2 \tilde{I} \right), \quad (C28)$$

$$[13(d)] = \tilde{m}_{\psi} \sigma_a \left(\delta Z_{\tilde{m}_{\psi}}^{(a)} \right) = \tilde{m}_{\psi} h^{-1} [10(b)]_a = \tilde{m}_{\psi} \sigma_a \left(-(d + \xi - 1) e^2 \tilde{I} \right). \quad (C29)$$

Only the ϕ field mass correction requires a new computation

$$\begin{aligned}
 [13(e)] &= m_{\phi}^2 \delta_{ab} \left(\delta Z_{m_{\phi}^2}^{(\phi)} \right) = \frac{1}{2} 8\lambda (\delta_{ab}\delta_{cd} + \delta_{ac}\delta_{bd} + \delta_{ad}\delta_{bc}) (m_{\phi}^2 \delta_{cd}) \int (d\mathbf{k}) \frac{1}{k^4} \\
 &= m_{\phi}^2 \delta_{ab} (4(N_b + 2)\lambda) \tilde{I}. \quad (C30)
 \end{aligned}$$

3. Results

The renormalization constants are obtained by summing the corrections found above, $Z_{x_i} = 1 + \sum_{\Phi=\phi,\psi,a} \delta Z_{x_i}^{(\Phi)}$ where $x_i \in \{\psi, \phi, a, e, h, \lambda\}$. In turn, this allows us to obtain the coefficients $\gamma_{x_i} = -d \ln Z_{x_i} / d\ln \approx -dZ_{x_i} / d\ln$ defined

in the main text in Eq. (81) which are given by

$$\gamma_\phi = 2N_f h^2, \quad (\text{C31})$$

$$\gamma_\psi = \left(d - 5 + \frac{4}{d} + \xi\right) e^2 + N_b \left(\frac{d-2}{d}\right) h^2, \quad (\text{C32})$$

$$\gamma_a = \frac{4N_f}{3} e^2, \quad (\text{C33})$$

$$\gamma_e = \gamma_\psi, \quad (\text{C34})$$

$$\gamma_h = (d + \xi - 1) e^2 + (N_b - 2) h^2, \quad (\text{C35})$$

$$\gamma_\lambda = -4(N_b + 8) \lambda + N_f h^4 \lambda^{-1}, \quad (\text{C36})$$

$$\gamma_{m_\phi^2} = -4(N_b + 2) \lambda, \quad (\text{C37})$$

$$\gamma_{m_\psi} = (d + \xi - 1) e^2 - N_b h^2, \quad (\text{C38})$$

$$\gamma_{\tilde{m}_\psi} = (d + \xi - 1) e^2 + (N_b - 2) h^2, \quad (\text{C39})$$

where we have eliminated the loop integral factor by rescaling the coupling constants

$$(e^2, h^2, \lambda) \rightarrow \left(\frac{\int d\Omega_{d-1}}{(2\pi)^d} \Lambda^{d-4} \right)^{-1} (e^2, h^2, \lambda). \quad (\text{C40})$$
